The Aneto Glacier (Central Pyrenees) evolution from 1981 to 2022: ice loss observed from historic aerial image photogrammetry and ~~recent~~ remote sensing techniques

Ixeia Vidaller[1], Eñaut Izagirre[2], Luis Mariano del Rio[3], Esteban Alonso-González[4], Francisco Rojas-Heredia[1], Enrique Serrano[5], Ana Moreno[1], Juan Ignacio López-Moreno[1], Jesús Revuelto[1]

[1] Instituto Pirenaico de Ecología, Consejo Superior de Investigaciones Científicas (IPE-CSIC), Zaragoza, Spain

[2] Department of Geography, Prehistory and Archaeology, University of the Basque Country UPV/EHU, Vitoria-Gasteiz, Spain

[3] Department of Applied Physics, Escuela Politécnica Superior de Cáceres, University of Extremadura, Cáceres, Spain

[4] Centre d'Etudes Spatiales de la Biosphère, Université de Toulouse,CNRS/CNES/IRD/INRA/UPS, Toulouse, France

[5] Department of Geography, GIR PANGEA, University of Valladolid, Valladolid, Spain

Corresponding author: Ixeia Vidaller (ixeia@ipe.csic.es)

Abstract. The Aneto Glacier, although it may be considered a very small glacier (<0.5 km^2), is the largest glacier in the Pyrenees. Its ~~shrinkage and wastage~~surface and thickness loss have been continuous in recent decades, and there are signs of accelerated melting in recent years. In this study, thickness and surface losses ~~changes in the area and volume~~ of the Aneto Glacier from 1981 to 2022 are investigated using historical aerial imagery, airborne LiDAR point clouds, and UAV imagery. A GPR survey conducted in 2020, combined with data from photogrammetric analyses, allowed us to reconstruct the current ice thickness and also the existing ice distribution in 1981 and 2011. Over the last 41 years, the total ~~glaciated~~ glacierized area has ~~shrunk~~ decrease by 64.7% and the ice thickness has decreased, on average, by 30.5 m. The mean remaining ice thickness in autumn 2022 was 11.9 m, as against the mean thickness~~es~~ of 32.9 m, 19.2 m and 15.0 m reconstructed for 1981 and 2011 and observed in 2020 respectively. The results demonstrate the critical situation of the glacier, with an imminent segmentation into two smaller ice bodies and no evidence of an accumulation zone. We also found that the occurrence of an extremely hot and dry year, as observed in the 2021–2022 season, leads to a drastic degradation of the glacier, posing a high risk to the persistence of the Aneto Glacier, a situation that could extend to the rest of the Pyrenean glaciers in a relatively short time.

Keywords: Aneto Glacier, Pyrenees, LiDAR, Unmanned Aerial Vehicle (UAV), Historical Aerial Images, Ground Penetrating Radar (GPR)

1 Introduction

Glaciers are excellent indicators of climate variability and change because their evolution depends on the balance between snow accumulation during the cold period and ice/snow ablation during the warmest season (Braithwaite and Hughes, 2020).The Little Ice Age (LIA) represents the last cold pulse in almost all mountain ranges of the world (Solomina et al., 2016; García-Ruiz et al., 2020). As Grove (2004) and Oliva et al. (2018) point out, the LIA in the Pyrenees occurred during the period between the 14th and 19th centuries, in common with the rest of the Northern Hemisphere. Since ~1850, the LIA maximum, the climate has been warming and glaciers have been receding, albeit with brief periods of stabilization or even small advances (Zemp et al., 2015; Oliva et al., 2018). However, the nearly continuous ~~shrinkage and wastage~~surface and thickness losses ha~~ve~~s accelerated in recent decades (Vidaller et al., 2021), similar to what is observed in the majority of mountain ranges in the world (~~Huss and Hock, 2018;~~ Hugonnet et al., 2021). The rapid ~~shrinkage~~surface and thickness losses~~and wastage~~ are mainly due to a warming of more than 1.2°C between 1949 and 2010 (Cuadrat et al., 2018), which could be even higher in high-elevation areas, affecting snow accumulation and its duration above ground (López-Moreno et al., 2019; López-Moreno, 2005). Due to the small size of Pyrenean glaciers, their evolution has been strongly influenced by the topographic characteristics of the surrounding area (size and height of cirques, aspect, slope, snow avalanche corridors, etc~~.):~~.), as well as an interannual climatic control, they now also have a topoclimatic control (López-Moreno et al., 2006; Vidaller et al., 2021).

Consequently, the glacier ~~area~~surface loss in the Pyrenees is remarkable: there were 52 glaciers in 1850, 39 in 1984, and 21 in 2020, corresponding to an area of 2,060 ha (20.6 km²) in 1850, 810 ha (8.1 km²) in 1984, and 232 ha (2.3 km²) in 2020, representing a loss of 88.8% of the glaciated area (Arenillas-Parra et al., 2008; Rico et al., 2017; Vidaller et al., 2021). In terms of ice thickness ~~wastage~~loss, unlike surface loss~~area shrinkage~~, there is ~~in general~~generally a lack of information over a long period of time and with a sufficient resolution for small alpine glaciers (or very small glaciers). Recent studies identified an ice thickness loss of 6.3 m for the period 2011–2020 as the mean for all the glaciers in the Pyrenean massif (Vidaller et al., 2021). Specifically, at Monte Perdido Glacier, López-Moreno et al. (2019) reported ~~wastage~~ice thickness loss of 6.1 m for the period 2011–2017. In the case of the Ossoue Glacier, the ~~geodetic mass balance was~~ice thickness loss was −36.8 m~~31.3 ± 1.9 m w.e. (water equivalent)~~ for the period 1983–2013 and ~~−17.3 ± 2.9 m w.e.~~20.4 m for the period 2001–2013 (Marti et al., 2015). In the grid cell corresponding to the Pyrenean glaciers (1°×1° grids 42°N, 0°E and 42°N, 1°W) of Hugonnet et al. (2021) indicated a mean ice thinning rate of -0.96 m yr⁻¹for the period 2000-2019, which is very accurate considering the dataset characteristics, but it is much higher than the mean annual ice thickness loss found by Vidaller et al. (2021) of −0.70 m yr⁻¹, for a more recent study period (higher ice loss could be expected in the later period). This difference between both studies clearly shows the need of local studies as the present study or Vidaller et al., 2021 to validate large scale observations and also to reach more accurate estimations over shorter time periods.

The Aneto Glacier is one of the southernmost glaciers in Europe (Grunewald and Scheithauer, 2010), and is the largest in the Pyrenees although it is ~~considered~~a very small glacier (<0.5 km²) (Huss and Fischer, 2016). It is one of the most iconic of

Pyrenean glaciers, as it is located below the highest peak of the mountain range (Aneto peak, 3,404 metres above sea level (m a.s.l.)) and it forms part of the natural and cultural landscape of the Posets-Maladeta Natural Park, attracting mountaineers and tourist to this Park (Carvache-Franco et al., 2022; Carrascosa-López et al., 2021). Additionally, this glacier is part of the Natural Monument of the Pyrenean Glaciers (Lampre-Vitaller, 2003), having an additional ~~protection figure~~societal value for this natural landscape heritage. Unlike other alpine glaciers that are important water source in other mountain areas (Fountain and Tangborn, 1985; Braithwaite and Raper, 2002; Meier et al., 2007; Huss et al., 2017; Drenkhan et al., 202~~2~~3) the Aneto glacier, as all Pyrenean glaciers, has a minor (and nearly negligible) contribution to rivers discharge in this region (López-Moreno et al., 2020). However, the ice surface loss~~shrinkage~~ of Pyrenean glaciers has a clear impact on local erosion rates (Riihimaki et al., 2005), nutrient fluxes, biochemistry and macroinvertebrate communities (Snook and Milner, 2001; Brown et al., 2007) or the microbiology of these emblematic landscapes and in surrounding downstream areas. The knowledge gap of these processes in the southernmost glaciers of Europe encourages and justifies the ~~comprehension~~ analysis of their recent evolution. ~~This study aims to exploit the largest spatio-temporal dataset of glacier observations to analyse the current state of the highest and largest glacier of the Pyrenees, the Aneto Glacier, combining state of the art methodologies. The evidence of Pyrenean glaciers demise in the next decades, thoroughly exemplified by this glacier (Vidaller et al., 2021) have a twofold interest; anticipate the evolution which might be expected in other temperate mountain glaciers and also to show the fast consequences of Climate Change in mountain areas to the society.~~

Despite the Aneto Glacier has not been subjected to mass balance annual monitoring~~to systematic annual mass balance monitoring to date~~, two recent studies (Campos et al., 2021; Vidaller et al. 2021) have analysed ice thickness ~~variations~~loss for different time periods. Campos et al. (2021)~~, 'Modeling the Retreat of the Aneto Glacier (Spanish Pyrenees) since the Little Ice Age, and Its Accelerated Shrinkage over Recent Decades',~~. presented a reconstruction of the area, volume, ice thickness, and Equilibrium Line Altitude (ELA) of Aneto Glacier for different time periods from the LIA to 2017, using photo interpretations and satellite imagery to calculate surface and ice thickness ~~changes~~losses in Aneto G~~g~~lacier ~~area and volume~~. Ice ~~wastage~~thickness loss in that work was derived from a steady-state model assuming a plastic ice rheology, combined with some Ground Penetrating Radar (GPR) profiles from 2008 (Campos et al., 2021). On the other hand, Vidaller et al. (2021) determined changes in glacier area and thickness for the period 2011–2020 with high spatial resolution in the 24 Pyrenean glaciers (including Aneto Glacier). ~~Shrinkage~~Surface loss was determined based on satellite data and drone imagery, and the ice thickness loss ~~wastage~~was calculated by comparing 2011 and 2020 Digital Elevation Models (DEMs) (from Laser Imaging Detection and Ranging (LiDAR) and unmanned aerial vehicle (UAV), respectively). The results of this work for Aneto Glacier reported a surface loss~~shrinkage~~ of 24.9% (69.3 ha (0.7 km^2) in 2011 and 50.0 ha (0.5 km^2) in 2020) and an average ice thickness ~~decrease~~loss of 8.5 m.

This study aims analysing the recent evolution of the highest and largest glacier of the Pyrenees, the Aneto Glacier, by using the longest temporal dataset of glacier thickness loss in the Pyrenees. In addition, this study permits to assess the impact of a single extreme warm ablation season (2022) on glacier evolution. Due to the very last stage in which Aneto glacier is, we report thickness and ice surface losses of this glacier from 1981 to 2022, to discern if the speed of changes accelerates (because

the existence of feedback processes) or slow down (because the remaining ice is progressively restricted to the most favourable areas), that has an inherent scientific interest and may be extrapolated to other mountain areas that will face a similar situation in the coming decades. The evidence for the demise of Pyrenean glaciers in the coming decades using the Aneto Glacier as an iconic example is also interest to highlight the dramatic consequences of rapid climate change in mountain areas. ~~In this study, we report the shrinkage and wastage of Aneto Glacier from 1981 to 2022 to build on the study of Vidaller et al. (2021) and try to determine the inflexion point at which the glacier shrinkage and wastage began its acceleration.~~ We use high-resolution 3D point clouds from 1981 (from Structure-from-Motion (SfM) methods exploiting historical aerial photographs), 2011 (from Spanish National Geographic Institute (IGN) LiDAR survey), 2020, 2021, and 2022 (from SfM methods using UAV flights). In addition, 2020 ice thickness was estimated from an intensive GPR survey conducted in July ~~2020~~of this year. The combination of the three techniques allows accurate reconstruction of the glacier ice thickness in 1981 and its evolution until today. Moreover, the current ice ~~volume~~ thickness and basal topography of the glacier could be determined. This information is critical for predicting the next changes in the glacier ~~, since sectors can be delineated using most grid-like techniques,~~ and the basal topography reveals sectors of likely lake formation after the ice disappears. The combination of these techniques provides an increase in knowledge over previous work because (1) we present data with high accuracy and lower uncertainty compared to previous studies and (2) we determine the evolution of Aneto Glacier for the longest period ~~ever~~ observed, by quantifying current ice thickness and basal topography, as well as the annual decrease in ice thickness from 1981 to 2022.

1.1 Study area

The Aneto Glacier is the largest glacier in the Pyrenees (~~47.9~~48.1 ha (0.48 km^2) in 2022), a mountain range where only four glaciers are larger than 10 ha. It is located in the Maladeta massif (Figure 1), on the northeast (NE) side, between the Maldito (3,354 m a.s.l.) and Aneto (3,404 m a.s.l.) peaks. The high elevation of this massif, with more than 40 peaks above 3,000 m a.s.l., has allowed the preservation of other smaller glaciers in the area (Eastern Maladeta and Tempestades) and ice patches (Western Maladeta, Coronas and Barrancs). In 2022, the Aneto Glacier consists of two bodies whose glacier front is at 3,026 m a.s.l. in the case of the main body and at 3,170 m a.s.l. in the case of the secondary body.
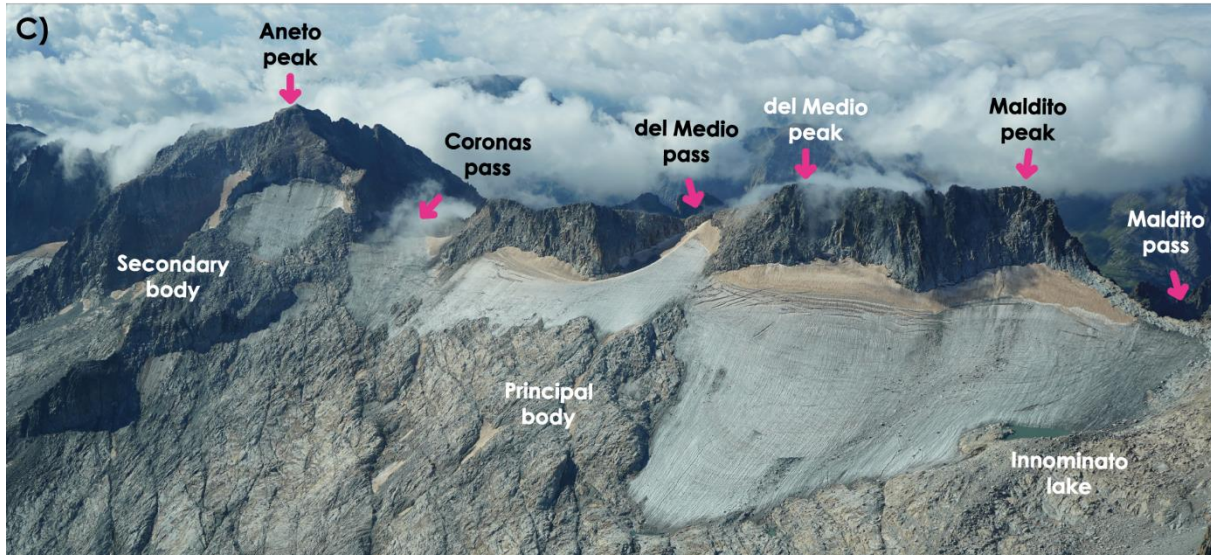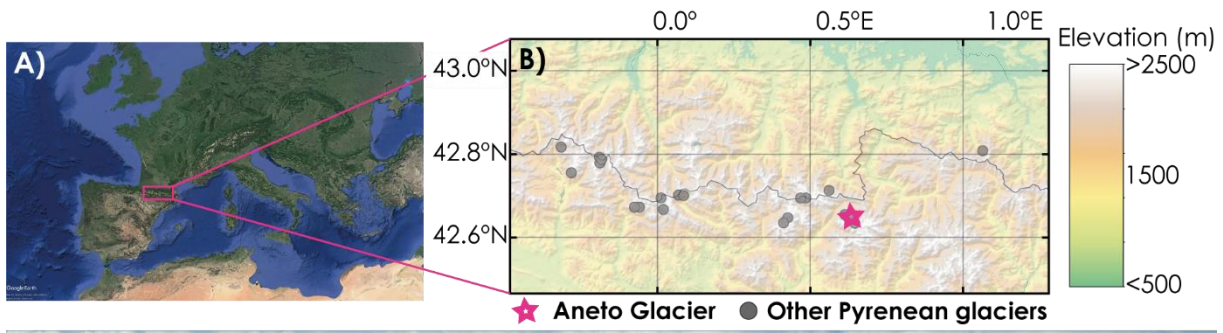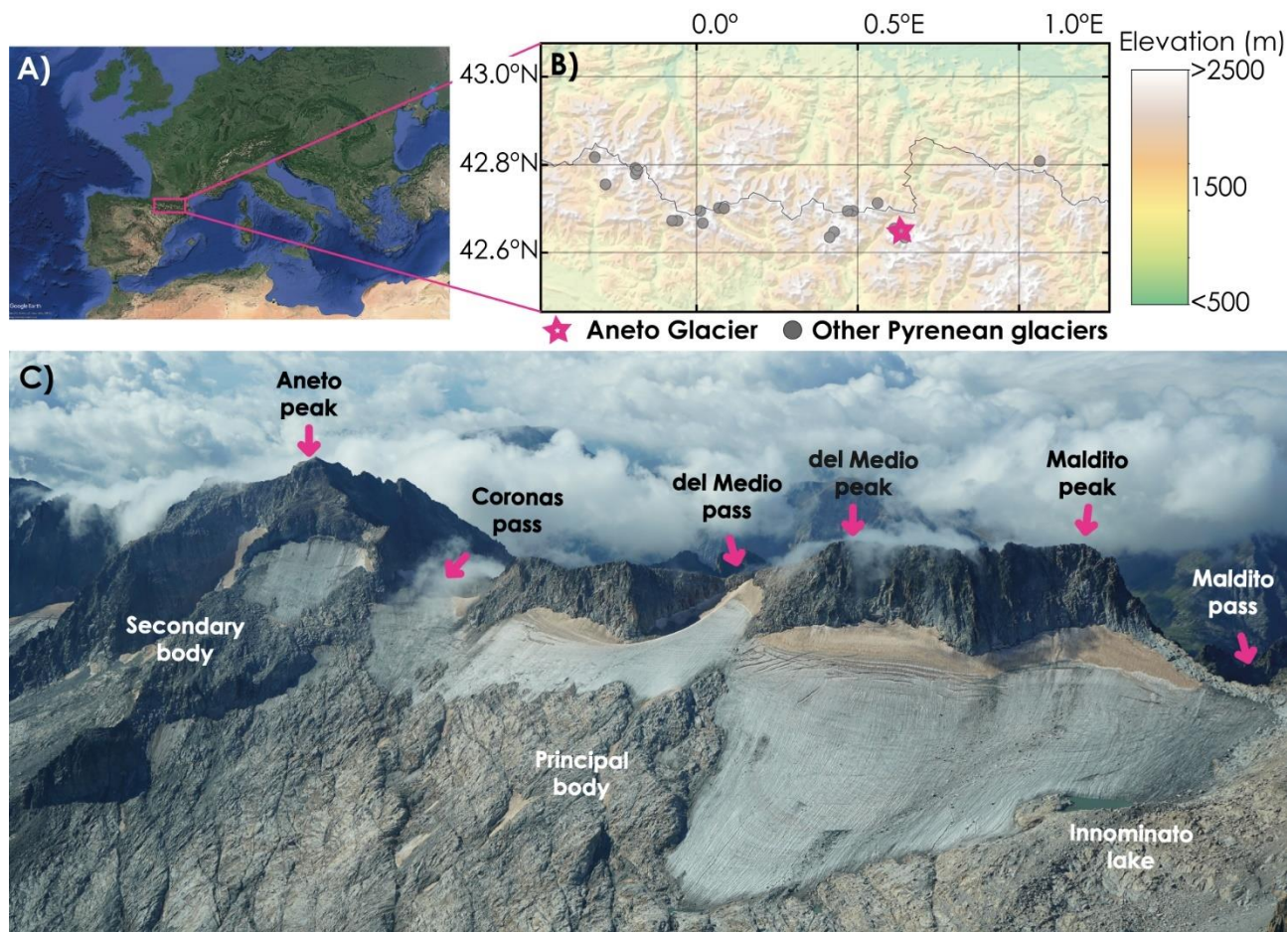
Figure 1: Location of the Aneto Glacier. (A) Map of Europe, with the pink rectangle delimiting the central part of the Pyrenees. © Google Maps (B) Topographic map of the central Pyrenees; the glaciers in this area are marked with grey dots and the location of the Aneto Glacier is marked with a pink star. (C) An aerial photo of Aneto Glacier in summer 2021. The main reliefs surrounding the glacier are indicated.

In this area, the 0°C mean annual isotherm ranges from 2,700 to 3,000 m a.s.l. (Jomelli et al., 2020), and the mean annual precipitation is about 2,000 mm, with winter and spring being the wettest seasons (Buisan et al., 2015). Mean annual temperature for the period 2007-2022 was 4.6 ℃ at the weather station of Renclusa hut (2,140 m a.s.l.), meanwhile the mean temperature for the same period in the ablation season (June-September) was 11.6 ℃. 2022 was an especially warm year, in which annual mean temperature was 5.2 ℃ and the summer mean temperature was 12.1 ℃ (data from the AEMET database). There are two weather stations in this area. One is located at Renclusa hut (2,140 m a.s.l.), where the maximum and minimum mean annual temperatures are 7 °C and 0.5°C, respectively, the maximum annual snow depth averages 4 m, and annual precipitation exceeds 1,300 mm (data from the AEMET database). The other station is located closer to Aneto summit, at 3,008 m a.s.l. since 2018 (data from the Aragon Government and the Natural monument of Pyrenean Glaciers database); the mean annual temperature there was −1.4°C (maximum of 15.4°C and minimum of −21.0°C) and the maximum snow thickness was 2.8 m (the station is in a windy location, so snow accumulation is often limited by wind redistribution).

2 Data and methods

2.1 Imagery processing and DEM generation

140 **2.1.1 Historical aerial imagery**

The earliest imagery dataset exploited here (1981 DEM) dates from September 1981. Aerial images were acquired by the Spanish National Geographic Institute (IGN) using analogue photogrammetric cameras (IGN, last accessed August 2022: http://centrodedescargas.cnig.es/CentroDescargas/index.jsp) aboard aircraft for national mapping surveys. The objective was to collect aerial photographs suitable to produce topographic maps of Spain at a scale of 1:50,000 and with contour intervals

145 of 20 m (named MTN50). The overlap was 60% front and 30% side. The camera, *Wild lens cone RC 10*, had a sensor of 230×230 mm, a lens of 15 UAG II and a focal length of 152.12 mm; thus, an average image scale of 1:30,000 was obtained, with a Ground Sampling Distance (GSD) between 0.35 and 0.18 m/pixel. For this study, the historical aerial imagery was rescanned ~~digitalized~~ at a resolution of 15 microns. A total of 18 aerial images of the Aneto massif were used, taken from the same flight in late summer 1981.

150 Historical survey imagery was processed using Structure-from-Motion (SfM) (Snavely et al., 2006) with Agisoft Metashape Professional v1.6.3 software (https://www.agisoft.com/), which has shown reliable results when used for processing historical images (Llena et al., 2018). Processing parameters were set according to official Agisoft guidelines (denser point clouds, Bundle Block Adjustment (BBA), internal and external camera parameter calibration; Agisoft Metashape version 1.5, 2019). The SfM routines enabled generation of a dense point cloud (2.4 pts/m^3), from which an orthomosaic with a resolution of 0.41

155 m (used to calculate the glacier area) and a geoid-corrected Digital Terrain Model (DTM) with a grid cell size of 1.58 m were derived.

The historical survey imagery processing included the following workflow: (1) alignment of each flight line's cameras (3 lines total); (2) assignment of Ground Control Points (GCPs) based on clearly visible features such as individual large boulders and trail crossings or mountain summits; (3) derivation of accurate geographic coordinates and elevation information of these later

160 GCPs using high-resolution satellite imagery (DigitalGlobe/GeoEye-1 imagery with 1 m resolution available through the QGIS service 'QuickMapServices') and a 2020 UAV flight as a reference DTM (Vidaller et al., 2021); (4) taking advantage of GCPs, camera positions were realigned and all images were merged in one chunk using Agisoft Metashape Professional. The georeferencing accuracy of DigitalGlobe's latest Very High Resolution (VHR) satellites (i.e., GeoEye-1 and WorldView-1/2/3/4) is between 1.0 and 5.0 m, which may be insufficient for many precise geodetic applications. To improve this, we

165 aligned the 1981 point cloud with that of 2020 using the ICP algorithm (Rajendra et al., 2014).

2.1.2 LiDAR survey

The 2011 high-resolution Digital Elevation Model (DEM) was derived from airborne LiDAR. The data were acquired in a flight of 9 November 2011, by the IGN (last accessed May 2022: http://centrodedescargas.cnig.es/CentroDescargas/index.jsp). The LiDAR device was a Leica ALS60 with a diode-pumped transmitter and a low-inertia/high-speed scanning mirror with a large aperture operating at a wavelength of 1,064 nm. The final georeferenced point cloud had an average density of 0.35 pts/m^3. This information was processed and accurately geolocated by the IGN, which provides free access to the final 3D point cloud.

2.1.3 Unmanned Aerial Vehicle (UAV) imagery

The 2020, 2021, and 2022 glacier surface DEMs were obtained using a fixed-wing UAV (SenseFly eBee-X) on 12 September 2020, 1 October 2021, and 10 September 2022, respectively. The UAV was equipped with a SenseFly 3D S.O.D.A. digital camera (20Mp resolution) and GPS receivers enabling PPK (Post-Processed Kinematic) positioning systems (positioning accuracy <0.05 m after post-processing). As in previous studies (e.g. Vidaller et al., 2021), the UAV images had an overlap of 70% front and 50% side (note that the 3D S.O.D.A. camera obtains images with a tilt of 30°) with a final ground sampling distance (GSD) of 2.8 cm/px. The UAV images were processed using Pix4Dmapper (Pix4D) SfM software, in which the calculation of BBA and internal and external camera parameters calibration was enabled (more details on data processing in Vidaller et al. (2021)). Although Agisoft metashape could be used for this SfM processing, we preferred to use the same protocol described in previous works with UAV at this site. ~~to reduce uncertainties.~~ Nonetheless comparison of point clouds from both SfM software (Pix4Dmapper and Agisoft metashape) shows equivalent accuracies ~~for working~~to work in ~~highly heterogeneous~~this area~~s~~ (Mölg and Bolch, 2017; Llena et al., 2020). Due to the three UAV acquisitions having the same acquisition protocol, and the GPS-PPK geolocation (images geolocation with deviations below 4 cm), the comparison of these three point clouds yielded negligible deviations (0.06 m) (Revuelto et al., 2021)~~.~~

2.2 In situ Ground Penetrating Radar (GPR), processing and data interpolation

GPR uses the transmission and rebound of electromagnetic pulses at different frequencies to determine ice thickness and glacier interfaces (rocks, bedrock basin, snow, etc.) (del Rio et al., 2014). Different works have studied the variation in ice thickness, surface area or volume on glaciers using different techniques, which highlight the importance of the methodology to be applied in each case, considering its scope and limitations (Procházková, 2019; Bohleber et al., 2017; Marcer et al., 2017; Fischer, 2009).

GPR fieldwork was conducted on 25–26 July 2020, using a Malå Geoscience radar system consisting of a ProEx control unit and a 100-MHz Rough Terrain Antenna (RTA). Occasionally several transects were also carried out with the 100 MHz shielded

antenna (see *Supplementary Material*). Georeferenced radargrams were created using the Atlas Link GNSS smart GPS antenna connected to the GPR, which were obtained in "time" tuning. A total of 32 georeferenced radargrams were recorded in the main glacier body in a common offset mode, corresponding to a length of 6.8 km and covering almost the entire glacier surface (more detailed information in *Supplementary Material, Figure S1*). The campaign was conducted during a period when the glacier surface was covered with snow, in order to allow safe displacement of the instrument and operators, thus hampering the observation of deeper ice layers. This required differentiation of the snow layer in post-processing to accurately quantify glacier thickness.

Radargrams were processed using ReflexW version 9.1.3 (Sandmeier Scientific Software), with the following workflow: (1) adjustment of the time origin (t=0) to coincide with the arrival of the first surface signal on the glacier. (2) Homogenization of the trace increment, since the acquisition of the radargrams with the RTA antenna was done in time mode and varied in each radargram depending on the speed of movement of the antenna on the ground (0.1 m/ns was fixed since this was the smallest value obtained in the radargrams). (3) Background removal. (4) Correction of the energy loss of the signal when penetrating the terrain by applying a gain factor of 0.2 (energy decay). (5) Application of a frequency bandpass filter so that only signals with frequencies between 50 and 200 MHz remain (the nominal frequency of the antenna is 100 MHz).

As a first approximation, 0.17 m/ns was set as the propagation velocity of the waves in the glacier to get a first idea of the thickness of the snow and ice layers in the radargram representation. Snow and ice layers must be defined from the radargrams to create a thickness model of both. To do this, the wave propagation velocities (RWV) in both media must be available beforehand. In a similar study on Monte Perdido Glacier, RWVs of 0.200 ± 0.005 m/ns for snow and 0.163 ± 0.007 m/ns for ice were obtained for the 500 MHz and 200 MHz antennas, respectively (López Moreno et al., 2019). The coherence of these velocities was checked in the 1054 radargram at the points where diffraction hyperbolas occur (plot of diffraction hyperbolas in *Supplementary Material, Figure S2*).

The distribution of the GPR data does not follow a homogeneous pattern; the GPR record tracks were distributed along parallel and perpendicular lines forming an irregular grid (*Figure S1 in Supplementary Material*). Therefore, to determine the thickness of the glacier over its entire extent, an interpolation method is required. For this type of data, the interpolation method used was the Radial Basis Function (RBF) as Otero-García (2008) recommended. Given the poor distribution of the data, after several tests, the best method is to work with 16 neighbours, two per octant (the closest points in each direction), in a circular area with a radius of 457.62 m to find, in the same way, again, as Otero-García (2008). The thickness for glacier limits in 2020 was established as zero m. To validate this interpolation method, the data were divided into two groups: Training with 70% of the sample and Test with the other 30%.

2.3 Glacier area outline, point cloud geolocation and glacier thickness ~~change~~ loss computation

The delineation of the Aneto Glacier ~~area~~ surface was done manually (Table S4 in *Supplementary Material)* in a GIS software (ArcGIS), considering: (1) the orthomosaic of the historical aerial imagery from 1981; (2) a RapidEye satellite image from 2011 and improved outlines from RGI (RGI Consortium, 2017); and (3) the orthomosaics derived from UAV flights in 2020,

2021, and 2022. Due to the small extent of these very small glaciers, the slope was considered in the calculation of glacier ~~area surface considered slope~~ to obtain the true glacier area (3D surface) rather than the 2D projection of glacier extent. This calculation is justified because the glaciers are strongly bound to wall cirques and these have a ~~strong slope~~steepness of 24.3° in 2020. When the slope is not~~; if this is not considered~~taken into account, the glacier ~~area~~surface ~~will be~~is underestimated (Vidaller et al., 2021). Otherwise the 2D area computation would also be affected by the changes in slope during the study period.

Data from DEM available for this work varied in accuracy. The most accurate geolocation is that of the UAV, which was used as a reference for the point cloud due to the PPK (Post Processed Kinematic) GPS geolocation technique (geolocation RMSE <0.05 m). This geolocation error is equivalent for the 2020, 2021, and 2022 point clouds (0.019 for 2020, 0.025 for 2021, and 0.021 for 2022, the differences were due to weather conditions). Based on the low magnitude of these geolocation errors, we assume that the error introduced in ice thickness differences is nearly negligible. 3D point cloud differences in ice free areas had RMSE below 0.02 m, (error computed following Vidaller et al., 2021 accuracy method).~~because the same acquisition protocol was used.~~ To coregister the LiDAR point cloud (2011) and the point cloud from the historical aerial imagery (1981), several areas of stable terrain such as ridges, peaks, polished surfaces, etc. were selected in these later point clouds and in the 2020 UAV-derived point cloud. These areas were evenly distributed around the glacier. A rotation and translation matrix was calculated for these areas to align (separately) the 1981 and 2011 point clouds with that of 2020 using an ICP algorithm (Rajendra et al., 2014), from Cloud Compare software (Girardeau-Montaut, 2016), in the same way as Vidaller et al. (2021). Subsequently, these matrices were applied to the entire point clouds to derive point clouds that were finally coregistered. Glacier ~~surface~~thickness ~~changes~~loss (normal surface differences, see *Supplementary Material* for more information) between these point clouds ~~dates~~ were computed using the Cloud ~~ ~~Compare tool M3C2 (James, 2017) to determine the differences (surface perpendicular) between the glacier surfaces observed in different years. Glacier change statistics were derived from this later comparison, calculated over the most recent (and smallest) glacier surface.

Glacier thickness loss ~~wastage~~ was determined by considering only data within the smallest (or more recent) ~~area~~surface of the glacier. When considering the oldest ~~area~~surface, there are zones of the glacier that are not present in the most recent acquisitions, so the ice thickness ~~change~~loss would be underestimated (Vidaller et al., 2021). The mass balance was calculated assuming a density conversion factor of 850±60 kg/m^3 (Huss, 2013). Thus, the specific mass balance presented in this study was determined considering the recent surface of the glacier.

With the aim of determining areas of future glacier lakes formation, the mountain basal topography was derived from the GPR interpolation and the 2020 UAV acquisition (subtraction of the 2020 glacier surface from the ice thickness interpolation from the GPR). Topographic Position Index (TPI) capable of identify terrain depressions at various search distances (Weiss et al., 2001). From this basal topography, the ~~Topographic Position Index~~TPI (~~TPI;~~ de Reu et al., 2013) was derived for 70, 100, 150 and 200 m search distances ~~was derived~~ to describe depression areas that potentially favour~~ing~~ future lake ~~areas~~formation. This index has ~~already~~ been used previously in studies of debris-covered glaciers (Westoby et al., 2020)~~.~~ to determine areas ~~with~~of potential debris accumulation~~ of rocks~~, but as far as the authors are aware~~know~~, this is the first time this index has been

used~~exploited~~ to determine areas of potential lake formation following the retreat of ~~after~~ mountain glaciers ~~retreat~~. In addition, overdeepenings detected by TPI were corroborated using the longitudinal GPR radargrams.

2.4 Correction and accuracy assessment

GPR ice thickness measurements with a 100-MHz RTA antenna are subject to intrinsic error. Assuming a RWV velocity for ice of 0.163 m/ns, the λ-value is 1.63 m, so the minimum spatial resolution is $\lambda/2 = 0.815$ m. Summing this uncertainty for snow and ice gives a thickness resolution of 1 m for this delineation. Thus, the uncertainty in the determination of the ice layer thickness is 1.8 m.

To check the coherence of the determined thicknesses, a test was performed at all intersections between transects to detect any inconsistencies in the values. At these 28 intersections, the average difference is 1.6 ± 1.6 (σ) m, with some outliers of 3–5 m (Table S2 in *Supplementary Material*). This value is consistent with the uncertainty associated with RWV velocity and ice layers' delineation (1.8 m). The lengths of the radargrams were determined using ReflexW from the GPS coordinates coupled to the GPR (see *Supplementary Material* for more details). General GPR uncertainty in ice thickness was determined considering different velocities for temperate ice in the transects (1043, 1062 and 1073). Based on existing literature (Jimenez, 2016; López-Moreno et al., 2018), we assumed 0.2 m/ns in the snow and between 0.157 and 0.186 m/ns into the ice. With these velocities, mean and maximum ice thickness were determined for each transect (Table S3 in *Supplementary Material*). As a result, mean ice thickness variation that could be derived from different velocity into the temperate ice would fit in the range of the estimated margin of error band (< 1.6 m) and smaller than the uncertainties obtained from the differences in thickness at transect crossings (< 1.8 m).

To validate the interpolation of glacier thicknesses, 30% of the GPR data were randomly selected and the remaining 70% of the GPR dataset was used for the interpolation (Otero García, 2008). The mean error between the interpolated thickness and the thickness observed with the GPR was 0.0018 m, and the RMSE was 0.3021 m.

The delineation of glacier boundaries also has some uncertainty due to pixel size, geometric correction, visual identification, and the presence of residual snow or debris cover at the glacier boundaries. ~~This~~ The surface uncertainty is 0.048 ha (0.0004~~848×10⁻⁴~~ km^2) for Aneto Glacier (Vidaller et al., 2021) in the case of the glacier surface of 2011, 2020, 2021 and 2022; the uncertainty error of the 1981 glacier outline is 0.58 ha (0.0058 km^2)~~.~~

The coregistration of point clouds from historical aerial imagery and LiDAR survey with UAV surveys was tested in a buffer zone around the glacier, always using snow- and ice-free zones in both years of comparison. This means that the comparison of the 1981 and 2020 point clouds was performed in a buffer zone with a 300% larger extent than the ~~around the~~ 1981 glacier boundaries (over stable terrain); the coregistration error between the 2011 and 2020 point clouds was determined in the same way. In the first case for Aneto Glacier the RMSE is 0.06 m, in the second case 0.4 m (Vidaller et al., 2021).

3 Results

The extent of the Aneto Glacier has decreased significantly in the last few decades, from 135.7 ha (1.36 km^2) in 1981 to ~~47.9~~48.1 ha (0.48 km^2) in 2022, i.e. by −64.7%. The ~~shrinkage and wastage~~surface and thickness losses of the glacier continues, resulting in changes in area and the division of the glacier into two bodies. It is noteworthy~~remarkable~~ that the secondary body today shows signs of stagnant dynamics~~has no movement today~~ (*Supplementary Material Table S~~1~~5*).

~~**Table 1:** Main characteristics of the Aneto Glacier over the years of the study.~~

Year		Area (ha)	Glacier front (m a.s.l.)	Area changes since 1981 (%)	Area changes since 1981 (% yr^{-1})
~~1981~~		~~135.7~~	~~2,828~~	~~–~~	~~–~~
~~2011~~		~~69.3~~	~~2,939~~	~~−49.0~~	~~−1.6~~
~~2020~~	~~Principal~~	~~47.8~~	~~3,011~~	~~−61.7~~	~~−1.6~~
	~~Secondary~~	~~4.2~~	~~3,170~~		
~~2021~~	~~Principal~~	~~46.1~~	~~3,014~~	~~−63.1~~	~~−1.6~~
	~~Secondary~~	~~3.9~~	~~3,170~~		
~~2022~~	~~Principal~~	~~45.1~~	~~3,026~~	~~−64.7~~	~~−1.6~~
	~~Secondary~~	~~2.8~~	~~3,170~~		

In 1981, the ~~area~~ surface of Aneto Glacier was 135.7 ha (1.36 km^2) ~~ha~~; in 2011, the surface decreased~~area shrank~~ to 69.3 ha (0,69 km^2), a loss of 49.0%. Between 2015 and 2016, the Aneto Glacier divided into two bodies; in 2020 the main body was 47.8 ha (0.48 km^2) and the secondary body was 4.2 ha (0.04 km^2), a total of 52.0 ha (0.52 km^2). Table S~~1~~5 in *Supplementary Material* ~~results~~ show~~s~~ that in the last 40 years the losses were 63.1% of its ~~area~~ surface (−1.6% yr^{-1}). In 2022, the ~~area~~ surface has ~~shrunk~~ decrease to ~~47.9~~48.1 ha (0.48 km^2) (~~45.1~~44.6 ha (0.45 km^2) for the main body and ~~2.8~~3.52 ha (0.03 km^2) for the secondary body), a decrease of 64.7% compared to 1981 (Figure 2). This decrease represents a retreat of the lowest glacier front (the front of the main body) from 2,828 m a.s.l. in 1981 to 2,939 m a.s.l. in 2011, 3,011 m a.s.l. in 2020, 3,014 m a.s.l. in 2021, and 3,026 m a.s.l. in 2022.
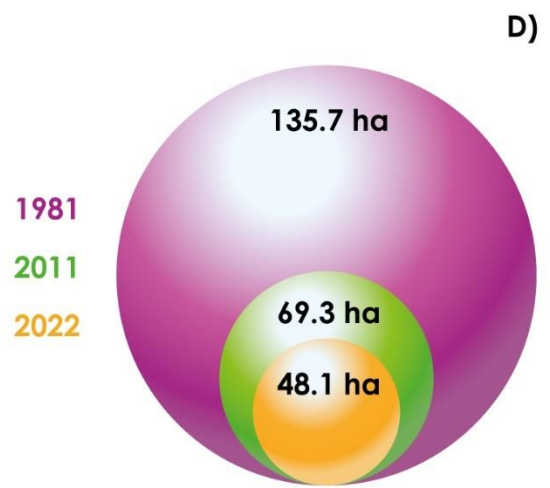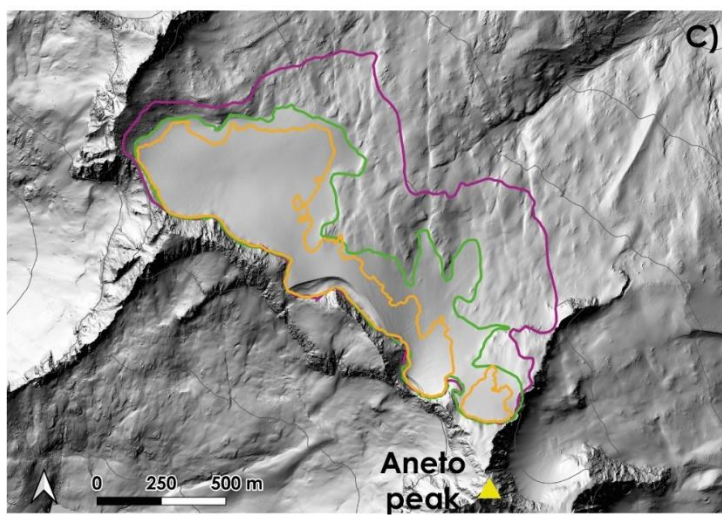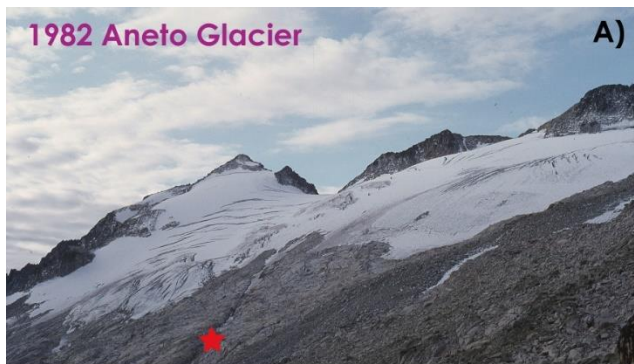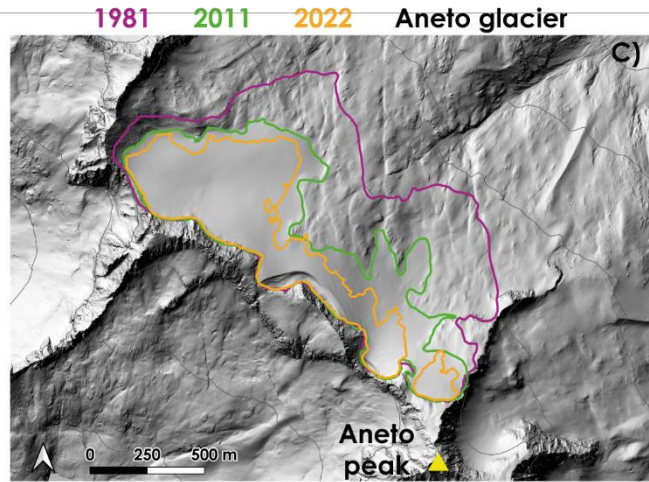
Figure 2: Appearance of the Aneto Glacier during the study period. (A) Photo (Fernando Biarge, Fototeca DPH) corresponding to Aneto Glacier in 1982. (B) Photo corresponding to Aneto Glacier in 2022. The red stars refer to the same location in both photos. (C) Map showing differences in the area of the glacier during the study period; the purple line delineates the extent of the glacier in 1981, the green line in 2011, and the orange line in 2020. The shading of the terrain was calculated from the 2011 LiDAR. The yellow triangle represents the summit of Aneto peak. (D) Cumulative area changes plot of the Aneto Glacier for the years 1981 (purple), 2011 (green) and 2022 (orange).

A comparison of the 1981 and 2022 point clouds (difference calculated normal to surface) shows a mean ice thickness loss of 30.51 m (Figure 3 and Figure S3 and S4 in *Supplementary Material*) in this period and considering only the area occupied by the glacier in 2022 (considering the 1981 glacier extent, the ice thickness loss is 24.1 m; and considering height surface changes the losses are 45.3 m (for more information see Table S6 and Figure S4 in *Supplementary Material*)). Note these mean ice thicknesses loss, are the mean value of differences in glacier surfaces (normally computed) for the entire period computed. This means that the glacier lost on average 0.6 m yr^{-1} over the entire glacier and 0.7 m yr^{-1} in the currently glaciated area during the 1981–2022 period. The thickness losses are not evenly distributed. The highest ice thickness ~~variations~~ loss is~~are~~ in the middle of the main body, while the lowest ~~variations~~ changes are in the secondary body (Figure 3A). More than 41% of the 2022 glacier area has lost more than the mean (30.5 m) (Figure 3B).

The results indicate an acceleration in glacier ice thickness loss ~~wastage~~ in the last decade. The mean ice thickness loss for the period 1981–2011 ~~is~~ was 17.8 m (0.6 m yr^{-1}) and 12.6 m (1.1 m yr^{-1}) for the period 2011–2022, representing an increase of ice thickness loss ~~wastage~~ in the later period of 200% compared to 1981–2011. The available information for the 2020–2021 and 2021–2022 annual comparisons highlights the high interannual variability of ice thickness loss, with mean ice thickness ~~decreases~~ loss of 1.5 m and 3.2 m, respectively. As for the specific mass balance, the ~~losses~~ changes are -0.6 m w.e. yr^{-1} for the period 1981–2022, -0.5 m w.e. yr^{-1} for the period 1981–2011, -1.0 m w.e. yr^{-1} for the period 2011–2022, -1.2 m w.e. yr^{-1} for the period 2020–2021, and -2.7 m w.e. yr^{-1} for the period 2021–2022 (data always calculated within the most recent glacier surface).
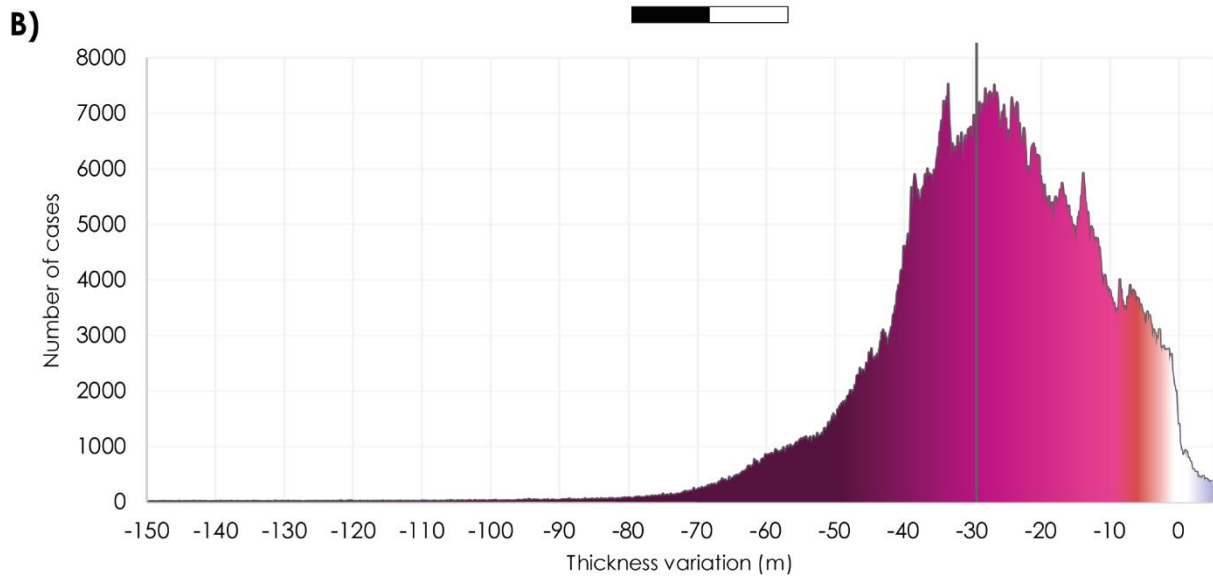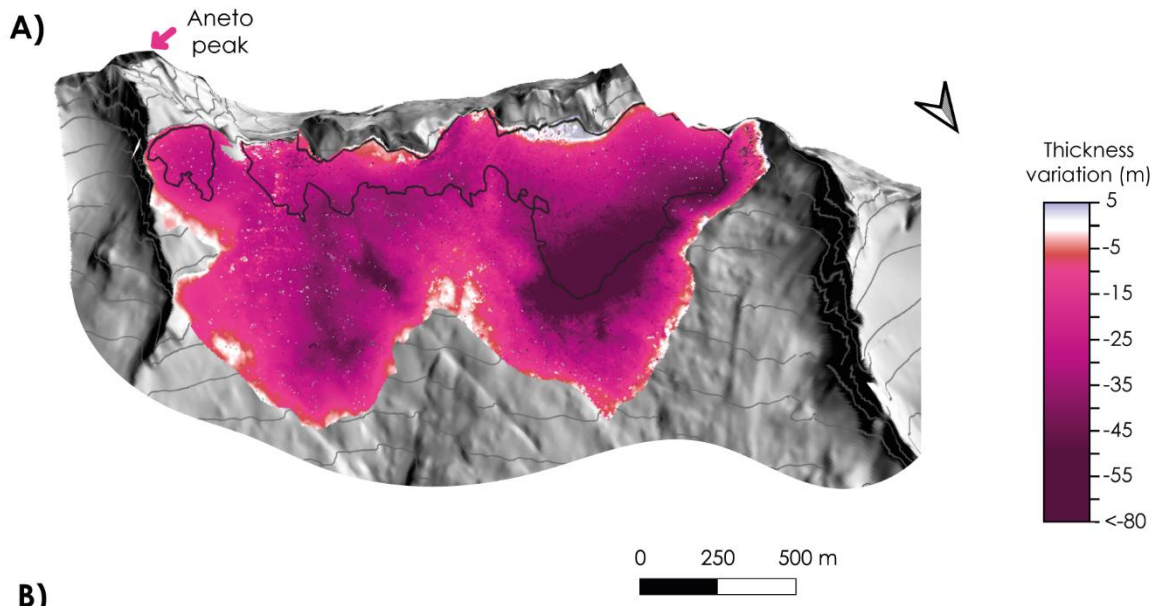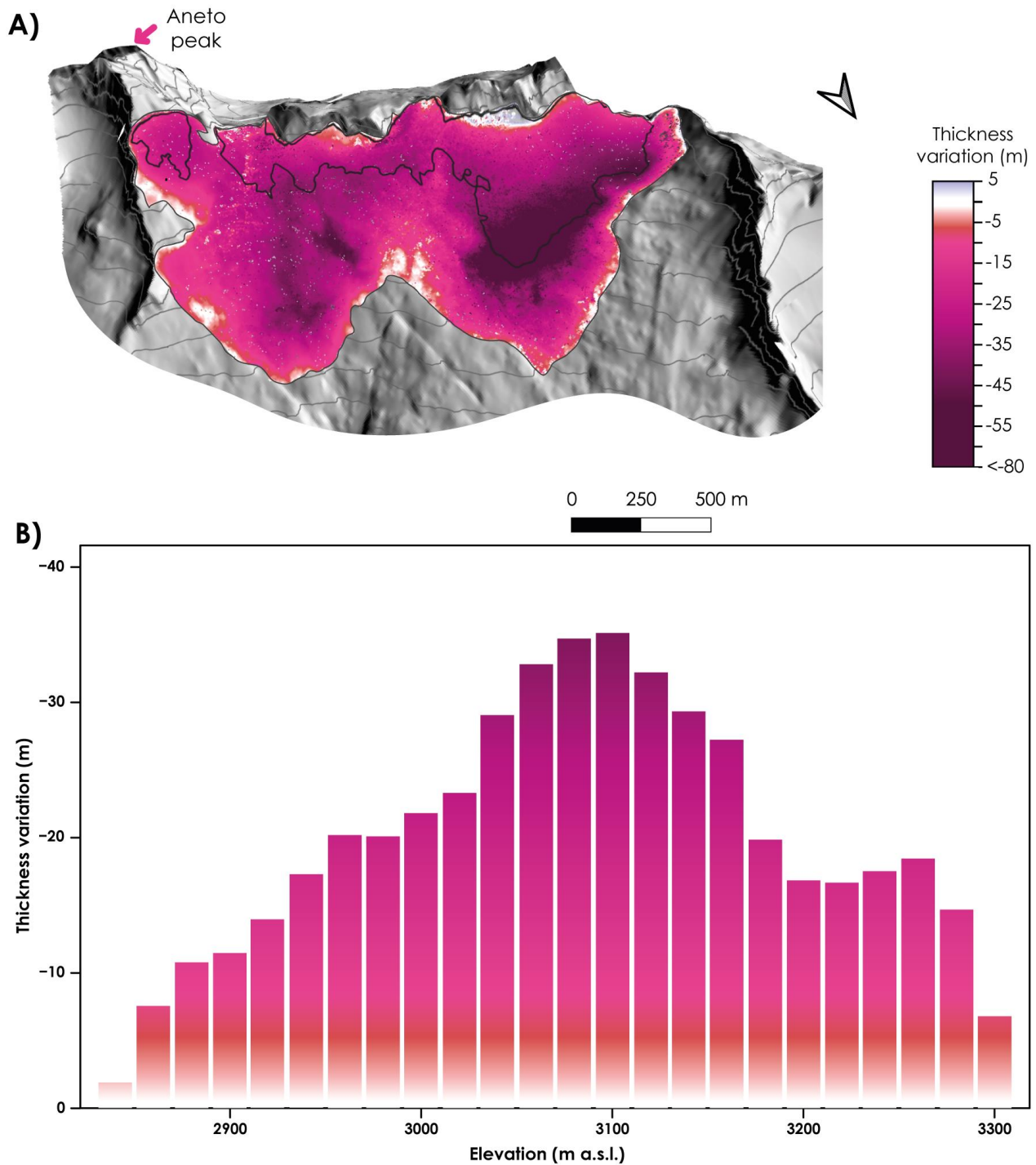
Figure 3: (A) Thickness ~~change~~ loss of Aneto Glacier from 1981 to 2022. In the upper map, the black line delineates the glacier in ~~2020~~2022 while grey line represents the glacier in 1981. The arrow indicates the north direction (see Supplementary Material Figure S3 the maps for

335

The GPR survey of the main body of the glacier in 2020 reveals a mean glacier thickness of 15.0 m, with a maximum glacier thickness of 44.7 m (Figure 4A). This maximum glacier thickness was measured in the western part of the glacier, near t~~he~~oe Maldito (3,354 m a.s.l.) and Del Medio (3,349 m a.s.l.) peaks. The greatest thickness was measured in the upper parts of the

340 glaciers in the elevation range between 3,200 and 3,350 m a.s.l. (Figure 4A and 4B). In some elevation ranges (between 3,100 m and 3,180 m a.s.l.), the glacier thickness is lower than expected, considering the trend of increase with increasing elevation. This is mainly due to the presence of a relatively thick sector (up to 39 m) between 3,000 and 3,100 m in the western part of the glacier, which affects the mean values observed in this elevation range. Figure 4A also shows the presence of very narrow and shallow ice sectors (light blue areas) adjacent to the cirque wall in two places, indicating an imminent separation of the

345 glacier into three ice bodies.
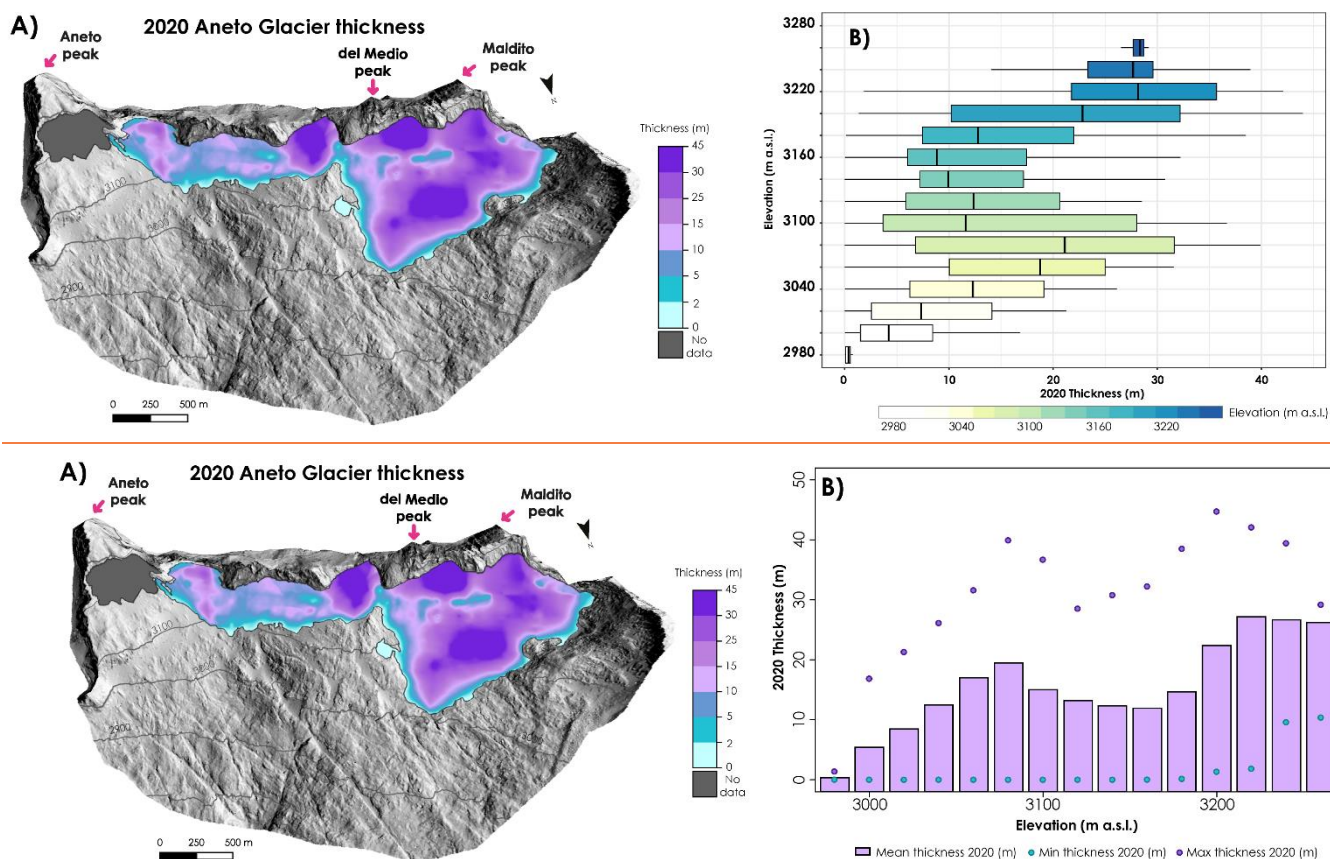
Figure 4: Ice thickness of Aneto Glacier in 2020. In map (A), the blue colour represents the zones of lesser ice thickness that are about to disappear, in contrast to the purple colours that represent the greatest ice thickness. The secondary body of the Aneto Glacier is coloured

350 grey because no data are available for this glacier body and therefore no interpolation is possible. The ~~diagram~~ boxplot (B) shows the mean glacier thickness in 2020 for each elevation band (20 m).~~as a function of the 20 m elevation levels. The bars describe the mean thickness,~~

the blue dots the minimum thickness, and the purple dots the maximum thickness of the individual elevation levels. A GPR profile is show in Supplementary Material as example of longitudinal radargram (SE-NW) of the glacier (Figure S5 in Supplementary Material).

355 By combining information on glacier thickness derived from the 2020 GPR observation with thickness losses estimated (with UAV and historical images) for 2011–2020 and 1981–2020, as well as those observed in subsequent periods (2020–2022) with UAV, ice thicknesses for 1981, 2011 and 2022 were reconstructed (Figure 5). In 1981 (Figure 5A), the pattern of ice thickness distribution shows some differences compared to recent periods. In 1981, the maximum glacier thickness was found in the middle elevations of the western part, where ice thickness reached 90 m. Below del Medio pass, the glacier thickness was also very highthick, almost 70 m. In 1981, the maximum thickness was 96.5 m, and the mean thickness of the glacier was 32.9 m.

360 In 2011 (Figure 5B), the distribution pattern of ice thickness on Aneto Glacier is very similar to that of 2020 (Figure 4A); maximum ice thickness was measured below the Maldito peak and in the lower western part of the glacier. The maximum ice thickness at that time was 52.5 m, while the mean ice thickness of the glacier was 19.2 m. In 2022 (Figure 5C), the ice thickness distribution has had not changed markedly, and the greatest thickness continues also wasto be under the Maldito pass and peak, and in the middle of the main body of Aneto Glacier. In this latter year, the average ice thickness is was 11.9 m, and the

365 maximum ice thickness is was 44.0 m, but although the maximum ice thickness exceeds exceeded 44 m, 43.0% of Aneto Glacier in 2022 has had an ice thickness of less than 10 m.
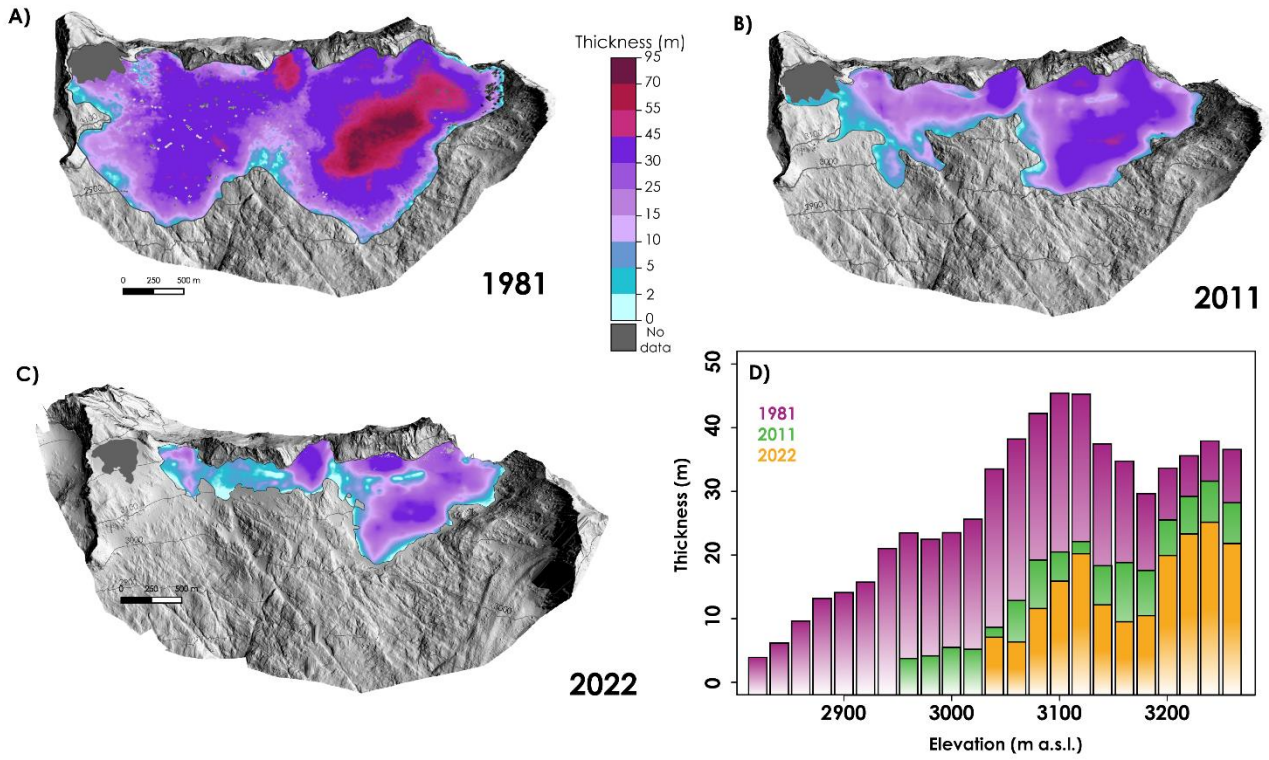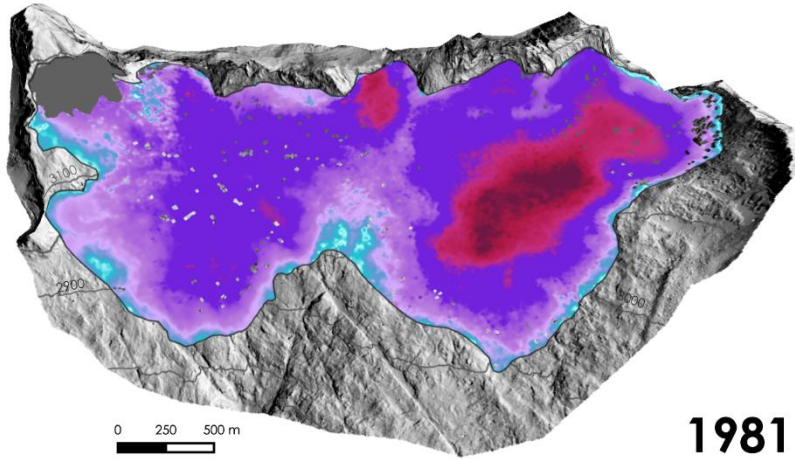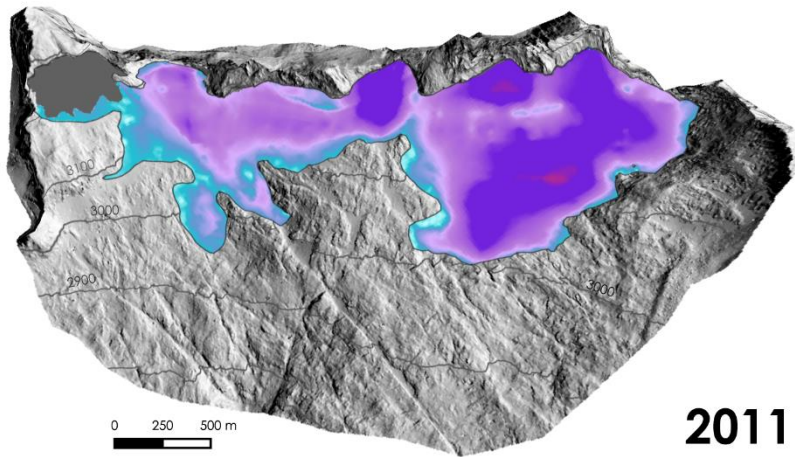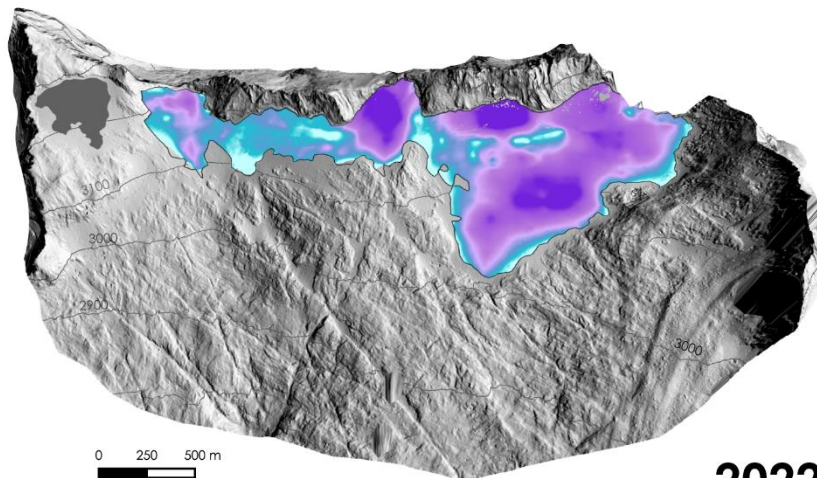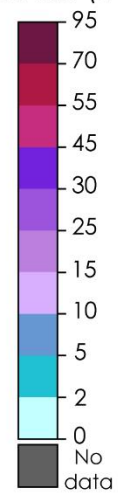
370 **Figure 5:** Reconstruction of the ice thickness of Aneto Glacier at different times during the study period. (A) shows the thickness in 1981, (B) shows the thickness in 2011, and (C) shows the thickness in 2022. The blue colour represents the zones of lower ice thickness that are about to disappear, in contrast to the red colours that represent the greatest ice thickness. The secondary body of the Aneto Glacier is coloured grey because no data are available for this glacier body and therefore no interpolation is possible. (D) Comparison of the thickness of Aneto Glacier in 1981, 2011 and 2022, structures in elevation bands of 20 m.

375 ~~As is well known, g~~Glaciers erode the surface beneath the ice mass so that the subglacial topography is not a flat surface (Palacios et al, 2020). Glacial erosion creates thresholds and depressions, which in some cases are filled by meltwater from the glacier, forming glacial lakes (Shugar et al., 2020; Yao et al., 2018). This is the case with Ibón Innominato, a new small proglacial lake formed in 2015 as a result of the retreat of the Aneto Glacier. Today, it is the highest mountain lake in the Pyrenees (3,150 m a.s.l.). Due to the continuous ~~shrinkage~~ surface loss of the glacier, this lake grows simultaneously with the

380 retreat of the Aneto Glacier, although it is ice-free only 3–4 months a year (July–October). In 2020, its area was 0.4 ha and in 2022 it was 0.5 ha, an increase in area of 26.5% for the period 2020–2022, mainly due to the frontal retreat of the Aneto Glacier by about 15.2 m.

~~Depression areas of the subglacial topography have been analysed through the TPI computed for four search distances (75, 100, 150, 200 m). This index has already been used in studies of debris-covered glaciers (Westoby et al., 2020).~~ ~~to determine~~

385 ~~areas with potential accumulation of rocks, but as far as the authors know, this is the first time this index has been exploited to determine areas of potential lake formation after mountain glaciers retreat.~~ The TPI spatial distribution depicts depression areas that could fill with water after the ice disappears (blue colours in Figure 6). For example, under the del Medio peak and "Medio" pass. a remarkable depression for 150 and 200 m search distances is observed. This spatial distribution of the lowest value of TPI is confirmed by radargram 1062 (Figure S5 in the *Supplementary Material*), in which the left side coincides with

390 the overdeepening area below del Medio pass and also with the second depression below Maldito peak. These areas nowadays have the highest ice thicknesses, and thus lakes could be found in these areas when the glacier has completely disappeared.
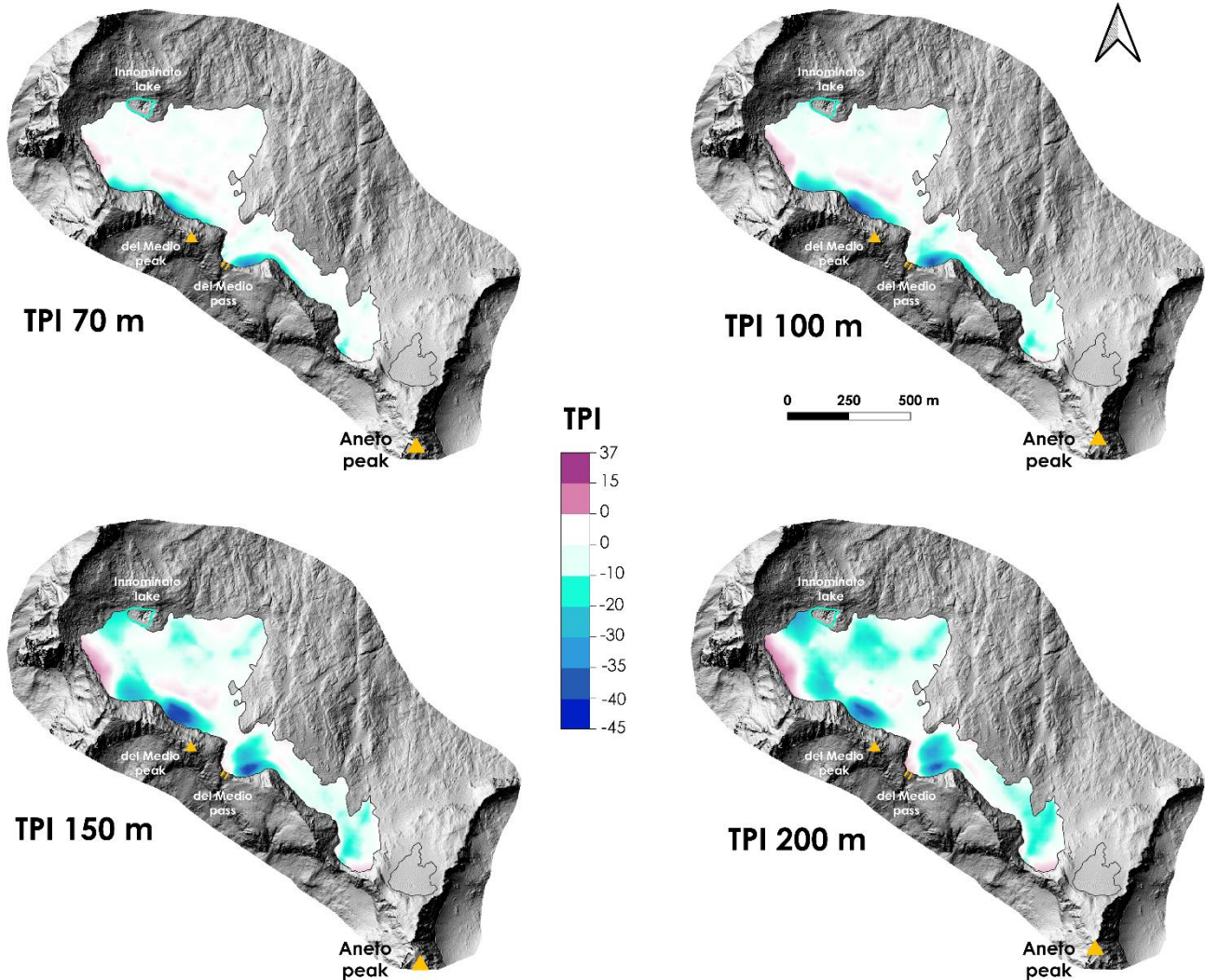
Figure 6: TPI 70, 100, 150 and 200 m based on the basal topography derived from the GPR data from 2020. Negative/positive values
(blue/red colours) represent locations that are lower/higher than their surroundings.

4 Discussion

4.1 Recent changes of the Aneto glacier: a foretaste of the future evolution of European glaciers

Annual ~~area~~ surface loss decreased uniformly over time ~~(−2.2 ha yr⁻¹, −2.2 ha yr⁻¹, −2.1 ha yr⁻¹, and −2.1 ha yr⁻¹ from 1981
to 2011, 2020, 2021, and 2022, respectively)~~ (-2.2 ha yr⁻¹). However, it must be noted that the relative changes are larger in the
latter years, since the losses occurring in the most recent period are measured with respect to a progressively smaller
~~area~~ surface. Thus, there ~~is~~ has been not ~~a~~ recent acceleration ~~of the~~ in ~~shrinkage~~ surface loss per year, but the relative ~~area~~
surface loss has increased. Oppositely, the rates of glacier thickness loss ~~Glacier thickness change rates~~ have increased during

the study period (−0.6 m yr⁻¹ from 1981 to 2011, and −~~0.6~~1.1 m yr⁻¹ from 2011 to 2022~~, −0.7 m yr⁻¹, and −0.7 m yr⁻¹ from 1981 to 2011, 2020, and 2022, respectively~~), indicating an acceleration of glacier ice thickness loss, especially in the last decade, and more pronounced in the last three years ~~volume wastage~~. In terms of specific mass balance (considering only changes at the smallest surface glacier, the most recent year of comparison), the losses are 0.6 m w.e. yr⁻¹ for the period 1981–2022, 0.5 m w.e. yr⁻¹ for the period 1981–2011, 1 m w.e. yr⁻¹ for the period 2011–2022, 1.2 m w.e. yr⁻¹ for the period 2020–2021, and 2.7 m w.e. yr⁻¹ for the period 2021–2022. Based on these results, two inflexion points can be identified, one after 2011 and another after 2020, in both cases the thickness loss has accelerated sharply. This ice thickness loss ~~wastage~~ is mainly accelerated (among other factors) by the fact that the accumulation zone over the glacier in summer is negligible, especially during very hot summers as 2022; and the ablation zone covers the entire glacier, as no ELA is observed for some years. Unfortunately, due to the small extent of this glacier no reliable satellite observations of sufficient resolution are available for Aneto Glacier ELA in late summer, and this absence of accumulation area is based on field work observations of UAV operators.

Various studies of other glaciers in the Pyrenees have also shown a continuous increase in glacier thickness and area loss~~es~~, with a high interannual variability but a clear negative trend over longer time periods. These works focused on Monte Perdido Glacier (López-Moreno et al., 2019), Ossoue Glacier (Gascoin and René, 2018), Maladeta Glacier (Pastor Argüello, 2013) and La Paul Glacier ~~(Rico et al., 2015)~~(Rico et al., 2015). Hugonnet et al. (2021) also determined a mean ice thinning of -0.96 m yr⁻¹ for the Pyrenean glaciers for the period 2000-2019. ~~Although this work focuses on the period 1981-2022, the glaciers of the Aneto-Maladeta massif had about 610 ha at the end of the LIA, so they lost about 338 ha from 1850 to 1984 (Rico et al., 2017).~~

The mean annual specific mass balance values of −0.6 m w.e. yr⁻¹ on Aneto Glacier determined for the period 1981–2022 are similar to those in other studies in the Alps, such as Davaze et al. (2020), who estimated an annual mass balance of −0.7 m w.e. yr⁻¹ from 2000 to 2016 for 239 Alpine glaciers. Similarly, Carturan et al. (2016) determined the mean annual mass balance of nine Italian glaciers from 2004 to 2013, which ranged from −1.8 to −0.8 m w.e. yr⁻¹. This is also supported by other climatic data showing an increase in air temperatures over the past century (Bolch et al., 2012; Rabatel et al., 2013), particularly a sharp rise in temperatures at high elevations and low latitudes (Vuille et al., 2008; Pepin et al., 2015), accompanied by a shorter duration of seasonal snow cover (Brown and Mote, 2009).

Vidaller et al. (2021) describe the changes in ice thickness of the Aneto Glacier (among other glaciers of the Pyrenees) based on an ice thickness decrease of 8.5 m during the period 2011–2020. Based on the ice thickness reconstruction data of the Aneto Glacier presented in this study, the mean ice thickness in 2020 was 15.0 m, while in 2011 it was 19.2 m, so the loss is 4.2 m. This difference is due to the fact that the mean ice thickness of 2011 was calculated based on the extent of 2011 and the ice thickness of 2020 was calculated based on the area of 2020, while in the case of Vidaller et al. (2021) the ice thickness loss ~~wastage~~ was calculated considering only the ice thickness loss~~es~~ within the glacier area of 2020. A similar problem exists when comparing the remaining ice thickness in 1981 (32.9 m) and in 2022 (11.9 m) with the ice thickness losses for the period 1981–2022 (30.5 m). Remaining ice thickness in 1981 is similar to those losses calculated for the period 1981–2022;

meanwhile the remaining average ice thickness was~~is~~ 11.9 m. The mean ice thickness for a particular year was calculated based on the extent observed for that year.

4.2 The importance of the methods

440 Remote sensing techniques have developed rapidly in recent years, allowing observation of the Earth's surface with a spatial resolution that was previously impossible. This work exploits historical aerial photographs to reconstruct a digital surface model for the year 1981 and provides a comparison to observe changes in landscapes and surfaces in detail.

Campos et al. (2021) calculated changes in Aneto Glacier from the LIA to 2017 using data from 1957, 1983, 2000, 2006, 2015, and 2017. In 1983, they reported an area of 103.2 ha (1.03 km^2), in contrast to the 135.7 ha (1.36 km^2) for 1981 described in

445 this work. The large difference may be due in part to the fact that they did not consider the slope angle of the terrain in their calculations (2D vs 3D surface). Nonetheless, considering our delineation, but ignoring the effect of slope angle on the area estimate, we would have reported a value of 115.5 ha (1.16 km^2) for 1981, which underestimates our value by 20%. This study also uses the National Fly photograms to convert to point clouds, accounting for stable GCP during the study period. This is a more accurate method because it avoids distortion of the *Plan Nacional de Ortofotografía Aérea* (PNOA) orthophotos used

450 by Campos et al. (2021), who acknowledge a source of uncertainty: "The extension for the 1983 stage should be considered with caution, due to the lower quality of the 1983 aerial Image~~.~~". The area determined in our study is closer to that reported by Arenillas-Parra et al. (2008), who reported an extent of 136 ha (1.36 km^2) for Aneto Glacier in 1982 based on aerial photographs of a specific flight in the glaciated areas of the Pyrenees.

The values of ice thickness from the GPR reported in Campos et al. (2021) also show significant differences not consistent

455 with our results. In 1994, the ERHIN programme estimated a maximum ice thickness of 52 m using 17 transects spaced 100 m apart (Arenillas-Parra et al., 2008; Jiménez-Vaquero, 2016). In 2008, those authors determined a maximum ice thickness of 30 m calculated from 31 GPR transects (Jiménez-Vaquero, 2016). Considering these data, Campos et al. (2021) reconstructed the subglacial topography of Aneto Glacier and based on this topography they determined a maximum ice thickness of 55 m for 1983, 37 m for 2006, and 29 m for 2015. These values are in stark contrast to our estimates (maximum 96.5 m in 1981,

460 52.5 m in 2011, 44.7 m in 2020, 43.5 m in 2021, and 41.8 m in 2022). Comparing the values of remaining thickness reported in 2008 (maximum ice thickness of 30 m (Jiménez-Vaquero, 2016)) and the rate of ice thickness loss ~~wastage~~ (-1.0 m yr^{-1}) established by Vidaller et al. (2021) for the period 2011–2020, the expected maximum thickness in 2020 would be 18 m instead of the 44.7 m we observed in 2020. Additionally, large areas currently covered by the glacier would be ice-free according to the previous ~~wastage~~ ice thickness loss estimates. Considering that we used comparable values for wave propagation velocity

465 of GPR signal to those used in the above-cited work, the differences between previous literature and the glacier thicknesses reported here are likely related to the more modern and accurate antennas used in our survey and the much denser net of transects conducted in the 2020 campaign. This methodology significantly reduces the uncertainties associated with the interpolation process, making the results obtained here more robust, and also permits a better understanding of the glacier's dynamic and its future behaviour.

4.3 Future perspectives

The rate of ~~shrinkage~~ surface and ice thickness losses ~~and wastage~~ calculated in this study and the reconstruction of ice thickness for the year 2022 indicate the critical situation of this glacier. There are no signs of slowdown in glacier surface and thickness losses rates ~~shrinkage and wastage~~; on the contrary, we have observed the high vulnerability of the Aneto Glacier to the occurrence of extremely hot summers in recent years, as 2022, when summer temperatures were 0.5°C above the mean for the period 2007-2022, according to ~~.~~ Renclusa station (2,140 m a.s.l.) and almost 2°C in general in the Iberian Peninsula (AEMET); thus, the continued loss of surface area and thickness could be due to an increase in temperature.

Taking into account the average current glacier thickness of 11.9 m, we can affirm that the Aneto Glacier is indeed in its terminal stage, with evident fragmentation into smaller ice bodies, the absence of a significant accumulation zone and obvious signs of ice stagnation. In this context, glacier ~~thinning~~ retreatment ~~and wastage~~ is exposing new areas of unconsolidated bedrock material (granite boulders and debris) and destabilizing cirque walls in many areas. This process is also accompanied by a degradation of surrounding wall permafrost (Rico et al., 2021). Under this situation the occurrence of unusual warm periods such as the observed in the 2021-2022 period, triggered hazardous rockfalls as were also noticed in other mountain areas (Huggel et al., 2010; Kellerer-Pirklbauer et al., 2012). This behaviour could also anticipate the behaviour of other temperate mountain glaciers in their final deglaciation phases.

Another aspect that determines the evolution of the Aneto Glacier is the darkening of the glacier surface. However, a detailed quantification of the darkening of the glacier surface and its effect on the energy and mass balance has not yet been carried out. Early spring/summer snowmelt and glacier thickness loss result in a grey/dark appearance of the glacier surface, which reduces the albedo effect and increases the absorption of thermal energy, leading to an acceleration of glacier surface and thickness losses (Shaw et al., 2021). ~~Early spring/summer snowmelt and glacier wastage result in a grey/dark appearance of the glacier surface, decreasing the albedo effect and increasing the heat absorption, which leads to an acceleration of the shrinkage and wastage of the glacier (Shaw et al., 2021; Xiao et al., 2023)Shaw et al., 'Glacier Albedo Reduction and Drought Effects in the Extratropical Andes, 1986–2020'~~. The obvious similarities with the remaining glaciers of the range suggest that the Pyrenees may become an ice-free mountain range in the next few decades.

The rise in temperature in recent decades, combined with a slight decrease in precipitation, has resulted in less snow accumulation during the winter months. This results in longer exposure of the glacier during the ablation season, which increases the melting of the glacier from year to year. Compared to Pyrenean glaciers that have a minimal contribution to water resources in downstram areas (López-Moreno et al., 2020~~b~~; Milner et al., 2017), changes in snowpack can lead to severe changes in the downstream water regime (García-Ruiz et al., 2011).

Also, of note is the presence and development of new proglacial lakes, as in the case of Ibón Innominato. This small lake is in constant change due to surface and thickness ~~shrinkage and wastage~~ of the glacier, where the retreat of the glacier front has opened new outlets beneath the glacier, and consequently the water level of the lake decreases. Similarly, as the Aneto Glacier shrinks, other lakes would be formed in the depression areas derived from the subglacial topography The presence of proglacial

lakes negatively affects the glacier's equilibrium by acting as an energy collector and accelerating the rate of thawing at the front of the glacier (Otto, 2019)~~Otto, 'Proglacial Lakes in High Mountain Environments'.~~. In addition, the dark appearance of
505 the glacier surface caused a decrease in albedo and therefore an increase in the ~~wastage and~~ surface and thickness losses~~shrinkage~~ of the glacier (Yue et al., 2020) ~~Yue et al., 'Variation in Albedo and Its Relationship With Surface Dust at Urumqi Glacier No. 1 in Tien Shan, China '.~~

On the other hand, the maximum ice thickness (>44 m) is located under Maldito pass, a protected area fed by avalanche channels and protected by the shadow of Maldito peak. In these areas, longer persistence of the ice body is expected.

510 The fast surface loss~~shrinkage~~ of Aneto Glacier in the last decades and the relatively low ice ~~thicknness~~thickness observed together with the potential development of new lakes, clearly show the consequences of climate change in mountain areas. Those changes happening nowadays in most mountain glaciers (Kääb et al., 2021; Barrand et al., 2017; DeBeer and Sharp, 2009) will have a major impact on mountain landscapes and ecosystems (Huss et al., 2017) showing the necessity of monitoring and understanding the recent fast evolution of these environments.

515 How long the glacier will maintain the main the ice movement and a surface greater than 2 ha to still be considered as a glacier is a very uncertain issue to be estimated. The duration of the glacier depends on several factors, such as the temperature evolution in the next few years, the evolution of precipitation (mainly snowfall in winter), the ability of the glacier to transport the debris fallen from the headwalls (and avoid the darkening of the surface), possible events of dust deposition (which may be frequent in winter and spring) and many other factors. In addition, according to the study by Vidaller et al. (2021), it is
520 possible that these very small glaciers, once they become smaller than 10 ha, will have a greater topoclimatic control, so their preservation could be prolonged if there are no more very hot summers, as in 2022. Otherwise, glacier extinction could be imminent if there are few summers like 2022 in the next decade. However, more detailed studies are needed to answer such a simple question, to reduce the uncertainty of observations, simulations and also to provide a deeper understanding of those processes that govern small and very small glaciers.

525 **5 Conclusions**

Aneto Glacier, although it is considered a very small glacier, is the largest glacier in the Pyrenees and also the largest in southern Europe. However, climate change has accelerated its disappearance, in common with other glaciers in the range. The evolution of close-range remote sensing techniques allowed us to observe the glacier surface in a very high level of detail that permits comparison between different years' surface (DEMs) of the glacier and evaluation of its changes.

530 For the period 1981–2022 the Aneto Glacier surface has diminished 64.7% (from 135.7 ha (1.36 km^2) to ~~47.9~~48.1 ha (0.48 km^2)) and its front has shifted from 2,828 m to 3,026 m. It has also been divided into two bodies between 2015 and 2016 and a proglacial lake has appeared in front of it in the last years. The annual rate of ~~area~~ surface loss~~decrease~~ has been constant over time (−2.2 ha yr^{-1} ~~and −2.1 ha yr^{-1} from 1981 to 2022 and from 2021 to 2022, respectively~~), but the relative surface loss~~shrinkage~~ of the glacier surface has increased during the study period.

The mean ice ~~thickness wastage~~thickness loss was estimated at 30.5 m ~~on average~~ for this 41-year period (with maximum losses over 80 m), with a specific mass balance of -0.7 m w.e. yr^{-1}. However, the annual ~~thickness~~specific mass balance ratio has been increasing, in fact quadrupled (-2.7 m w.e. yr^{-1} for the period 2021–2022) over the period 1981–2022. Using GPR measurements, we have estimated a mean of 44.7 m of ice thickness in 2020. GPR data and ice thickness loss estimated with UAV data have been used to infer the actual mean ice thickness, which ~~is~~ was 11.9 m. The ice thickness distribution shows areas around the glaciers with very little thickness (<2 m), so these zones are very close to becoming deglaciated during the coming summers.

The ~~shrinkage and wastage~~surface and thickness losses of Aneto Glacier indicate the critical situation of this ice mass. It is in its terminal stage, displaying fragmentation into smaller ice bodies and the presence of debris cover in some areas.

Acknowledgments:

This work was supported by the Interreg-POCTEFA project OPCC ADAPYR and Spanish Ministry of Economy and Competitiveness project "CGL2017-82216-R" and the Spanish Ministry of Science and Innovation "PID2020-113247RB-C21 and PID2021-124220ob-100/MARGISNOW". J. Revuelto has been supported by the IJC2018-036260-I (Juan de la Cierva I) and RYC2021-033859-I (Ramón y Cajal) projects. I. Vidaller is supported by the Grant FPU18/04978 and is studying the PhD programme in the University of Zaragoza. E. Izagirre is supported by the Grant PPGI19/02 (UPV/EHU) and the Consolidated Research Group IT1678-22 (Basque Country Government). Esteban Alonso-González has been funded by the CNES postdoctoral fellowship.

Funding:

We thank the Spanish National Geographic Institute (IGN) for the collection, archiving and distribution of the aerial photographs. We also thank the NextGIS/QuickMapServices plugin (Original Work Published in 2014), available online at https://github.com/nextgis/quickmapservices (accessed June 2, 2021). And to AEMET to share the climatic data of Renclusa hut.

Contributions:

Conceptualization, I.V., J.I.L.M., E.I., J.R..; methodology, I.V., E.I., L.M.dR., J.R.; software, I.V., E.I., J.R; validation, I.V., E.I., L.M.dR., J.R, J.I.L.M.; formal analysis, I.V., J.R., E.I., investigation, all authors.; resources, J.I.L.M.; data acquisition, all

authors; writing—original draft preparation, I.V..; writing—review and editing, all authors; visualization, I.V..; funding
565 acquisition, J.I.L.M. All authors have read and agreed to the published version of the manuscript.

References

Arenillas-Parra, M., Cobos-Campos, G., and Navarro-Caravallo, J.: Datos sobre la nieve y los glaciares en las
570 cordilleras españolas. El programa ERHIN (1984–2008), Ministerio., Madrid, 236 pp., 2008.

Barrand, N. E., Way, R. G., Bell, T., & Sharp, M. J.: (2017). Recent changes in area and thickness of Torngat Mountain
glaciers (northern Labrador, Canada)., The Cryosphere, 11(1), 157–168., https://doi.org/10.5194/tc-11-157-2017, 2017.

Bohleber, P., Sold, L., Hardy, D. R., Schwikowski, M., Klenk, P., Fischer, A., Sirguey, P., Cullen, N. J., Potocki, M.,
Hoffmann, H., and Mayewski, P.: Ground-penetrating radar reveals ice thickness and undisturbed englacial layers at
575 Kilimanjaro's Northern Ice Field, Cryosph., 11, 469–482, https://doi.org/10.5194/tc-11-469-2017, 2017.

Bolch, T., Kulkarni, A., Kääb, A., Huggel, C., Paul, F., Cogley, J. G., et al.: (2012). The State and Fate of Himalayan
Glaciers. Science, 336(6079), 310–314., https://doi.org/10.1126/science.1215828, 2012.

Braithwaite, R. J. and Hughes, P. D.: Regional geography of glacier mass balance variability over seven decades 1946–
2015, Front. Earth Sci., https://www.frontiersin.org/article/10.3389/feart.2020.00302, 2020.

580 Braithwaite, R. J., & Raper, S. C. B. : (2002). Glaciers and their contribution to sea level change. Physics and Chemistry
of the Earth, Parts A/B/C, 27(32), 1445–1454. https://doi.org/https://doi.org/10.1016/S1474-7065(02)00089-X, 2002.

Brown, L. E. E. E., Hannah, D. M., & Milner, A. M.: (2007). Vulnerability of alpine stream biodiversity to shrinking
glaciers and snowpacks., Global Change Biology, 13(5), 958–966., https://doi.org/https://doi.org/10.1111/j.1365-
2486.2007.01341.x, 2007.

585 Brown, R. D., & Mote, P. W.: (2009). The Response of Northern Hemisphere Snow Cover to a Changing Climate.,
Journal of Climate, 22(8), 2124–2145., https://doi.org/10.1175/2008JCLI2665.1, 2009.

Buisan, S. T., Saz, M. A., and López-Moreno, J. I.: Spatial and temporal variability of winter snow and precipitation
days in the western and central Spanish Pyrenees, Int. J. Climatol., 35, 259–274,
590 https://doi.org/https://doi.org/10.1002/joc.3978, 2015.

Campos, N., Alcalá-Reygosa, J., Watson, S. C., Kougkoulos, I., Quesada-Román, A., and Grima, N.: Modeling the
retreat of the Aneto Glacier (Spanish Pyrenees) since the Little Ice Age, and its accelerated shrinkage over recent decades, 31,
1315–1326, https://doi.org/10.1177/09596836211011678, 2021.

Carrascosa-López, C., Carvache-Franco, M., & Carvache-Franco, W.: (2021). Perceived Value and Its Predictive
595 Relationship with Satisfaction and Loyalty in Ecotourism: A Study in the Posets-Maladeta Natural Park in Spain.,

Sustainability, 13(14). https://doi.org/10.3390/su13147860, 2021

Carturan, L., Baroni, C., Brunetti, M., Carton, A., Dalla Fontana, G., Salvatore, M. C., Zanoner, T., and Zuecco, G.: Analysis of the mass balance time series of glaciers in the Italian Alps, Cryosphere, 10, 695–712, https://doi.org/10.5194/tc-10-695-2016, 2016.

600   Carvache-Franco, M., Carrascosa-López, C., & Carvache-Franco, W.: (2022). Market Segmentation by Motivations in Ecotourism: Application in the Posets-Maladeta Natural Park, Spain. Sustainability, 14(9). https://doi.org/10.3390/su14094892, 2022.

Cuadrat, J. M., Valero-Garcés, B., Moreno, A., Verfaillie, D., Galop, D., Rodríguez, E., Tejedor, E., Lostres, F. B.-, Soubeyroux, J.-M., Cunillera, J., García-Ruiz, J. M., López-Moreno, J. I., Trapero, L., Pons, M., Prohom, M., Saz, M. A., 605   González-Sampériz, P., Ramos, P., Amblar, P., Copons, R., Serrano-Notivoli, R., Gascoin, S., and Luna, Y.: El cambio climático en los Pirineos: impactos, vulnerabilidades y adaptación, OPCC, 149 pp., 2018.

Davaze, L., Rabatel, A., Dufour, A., Hugonnet, R., and Arnaud, Y.: Region-wide annual glacier surface mass balance for the European Alps from 2000 to 2016, 2020.

DeBeer, C. M., & Sharp, M. J.: (2009). Topographic influences on recent changes of very small glaciers in the 610   Monashee Mountains, British Columbia, Canada. Journal of Glaciology, 55(192), 691–700. https://doi.org/10.3189/002214309789470851, 2009.

Drenkhan, F., Buytaert, W., Mackay, J. D., Barrand, N. E., Hannah, D. M., & Huggel, C.: (2022). Looking beyond glaciers to understand mountain water security. Nature Sustainability. https://doi.org/10.1038/s41893-022-00996-4, 2023.

Fischer, A.: Calculation of glacier volume from sparse ice-thickness data, applied to Schaufelferner, Austria, J. Glaciol., 615   55, 453–460, https://doi.org/10.3189/002214309788816740, 2009.

Fountain, A. G., & Tangborn, W. V.: (1985). The Effect of Glaciers on Streamflow Variations. Water Resources Research, 21(4), 579–586. https://doi.org/https://doi.org/10.1029/WR021i004p00579, 1985.

García-Ruiz, J. M., Palacios, D., Andrés, N., and López-Moreno, J. I.: Neoglaciation in the Spanish Pyrenees: a multiproxy challenge, Mediterranean Geoscience Reviews, 2, 21–36, https://doi.org/10.1007/s42990-020-00022-9, 2020.

620   García-Ruiz, J. M., López-Moreno, J. I., Vicente-Serrano, S. M., Lasanta–Martínez, T., & Beguería, S.: (2011). Mediterranean water resources in a global change scenario. Earth-Science Reviews, 105(3), 121–139. https://doi.org/https://doi.org/10.1016/j.earscirev.2011.01.006, 2011.

Gascoin, S. and René, P.: Recent evolution of the Vignemale glaciers (2013–2017), Pirineos, 173, https://doi.org/10.3989/pirineos.2018.173004, 2018.

625   Girardeau-Montaut, D.: CloudCompare, Retrieved from CloudCompare https//www. danielgm. net/cc, 2016.

Grove, J. M.: Little ice ages: Ancient and modern, Routledge., London, 1–718 pp., https://doi.org/10.4324/9780203505205, 2004.

Grunewald, K. and Scheithauer, J.: Europe's southernmost glaciers: response and adaptation to climate change, Journal of Glaciology, 56, 129–142, https://doi.org/DOI: 10.3189/002214310791190947, 2010.

Huggel, C., Salzmann, N., Allen, S., Caplan-Auerbach, J., Fischer, L., Haeberli, W., et al.: (2010). Recent and future warm extreme events and high-mountain slope stability, Philosophical Transactions of the Royal Society A: Mathematical, Physical and Engineering Sciences, 368(1919), 2435–2459, https://doi.org/10.1098/rsta.2010.0078, 2010

Hugonnet, R., McNabb, R., Berthier, E., Menounos, B., Nuth, C., Girod, L., Farinotti, D., Huss, M., Dussaillant, I., Brun, F., and Kääb, A.: Accelerated global glacier mass loss in the early twenty-first century, Nature, 592, 726-731, https://doi.org/10.1038/s41586-021-03436-z, 2021.

Huss, M.: Density assumptions for converting geodetic glacier volume change to mass change, Cryosph., 7, 877–887, https://doi.org/10.5194/tc-7-877-2013, 2013.

Huss, M. and Fischer, M.: Sensitivity of very small glaciers in the Swiss Alps to future climate change, Front. Earth Scie., 4, https://www.frontiersin.org/article/10.3389/feart.2016.00034, 2016.

Huss, M. and Hock, R.: Global-scale hydrological response to future glacier mass loss, Nat Clim Chang, 8, https://doi.org/10.1038/s41558-017-0049-x, 2018.

Huss, M, Bookhagen, B., Huggel, C., Jacobsen, D., Bradley, R. S., Clague, J. J., et al.: (2017). Toward mountains without permanent snow and ice, Earth's Future, 5(5), 418–435, https://doi.org/https://doi.org/10.1002/2016EF000514, 2017.

James, M.: Precision maps and 3-D uncertainty-based topographic change detection with structure-from-motion photogrammetry, Earth Surf. Procss. and Landf, 42, 1769-1788, https://doi.org/10.1002/esp.4125, 2017.

Jiménez-Vaquero, C.: Cartografiado de la morfología subglaciar de La Maladeta y Aneto mediante georradar, Universitat Politècnica de València, 2016.

Jomelli, V., Chapron, E., Favier, V., Rinterknecht, V., Braucher, R., Tournier, N., Gascoin, S., Marti, R., Galop, D., Binet, S., Deschamps-Berger, C., Tissoux, H., Aumaitre, G., Bourlès, D. L., and Keddadouche, K.: Glacier fluctuations during the Late Glacial and Holocene on the Ariège valley, northern slope of the Pyrenees and reconstructed climatic conditions, Mediterr. Geosci. Rev., 2, 37–51, https://doi.org/10.1007/s42990-020-00018-5, 2020.

Kääb, A., Jacquemart, M., Gilbert, A., Leinss, S., Girod, L., Huggel, C., et al.: (2021). Sudden large-volume detachments of low-angle mountain glaciers – morefrequent than thought? The Cryosphere, 15(4), 1751–1785, https://doi.org/10.5194/tc-15-1751-2021, 2021.

Kellerer-Pirklbauer, A., Lieb, G. K., Avian, M., & Carrivick, J.: C (2012). climate change and rock fall events in high mountain areas: Numerous and extensive rock falls in 2007 at Mittlerer Burgstall, Central Austria, Geografiska Annaler: Series A, Physical Geography, 94(1), 59–78, https://doi.org/https://doi.org/10.1111/j.1468-0459.2011.00449.x, 2012

Lampre Vitaller, F.: (2003). *Monumentos Naturales de los Glaciares Pirenaicos*, Diputación General de Aragón, 36 pp., 2003.

Llena, M., Cavalli, M., Vericat, D., and Crema, S.: Assessing landscape changes associated to anthropic disturbances by means of the application of Structure from Motion photogrammetry using historical aerial imagery, Rendiconti Online Societa Geologica Italiana, 46, 74–81, https://doi.org/10.3301/ROL.2018.55, 2018.

665 Llena, M., Vericat, D., Martínez-Casasnovas, J. A., and Smith, M. W.: Geomorphic adjustments to multi-scale disturbances in a mountain river: A century of observations, Catena (Amst), 192, 104584, https://doi.org/https://doi.org/10.1016/j.catena.2020.104584, 2020.

López-Moreno, J. I.: Recent variations of snowpack depth in the central Spanish Pyrenees, Arct Antarct Alp Res, 37, 253–260, https://doi.org/10.1657/1523-0430(2005)037[0253:RVOSDI]2.0.CO;2, 2005.

670 López-Moreno, J. I., Nogués-Bravo, D., Chueca-Cía, J., and Julián-Andrés, A.: Change of topographic control on the extent of cirque glaciers since the Little Ice Age, Geophys Res Lett, 33, 1–5, https://doi.org/10.1029/2006GL028204, 2006.

López-Moreno, J. I., Alonso-González, E., Monserrat, O., del Río, L. M., Otero, J., Lapazaran, J., Luzi, G., Dematteis, N., Serreta, A., Rico, I., Serrano-Cañadas, E., Bartolomé, M., Moreno, A., Buisan, S., and Revuelto, J.: Ground-based remote-sensing techniques for diagnosis of the current state and recent evolution of the Monte Perdido Glacier, Spanish Pyrenees,

675 Journal of Glaciology, 65, 85–100, https://doi.org/10.1017/jog.2018.96, 2019.

López-Moreno, J. I., García-Ruiz, J. M., Vicente-Serrano, S. M., Alonso-González, E., Revuelto-Benedí, J., Rico, I., et al.: (2020). Critical discussion of: "A farewell to glaciers: Ecosystem services loss in the Spanish Pyrenees." Journal of Environmental Management. https://doi.org/10.1016/j.jenvman.2020.111247, 2020.

Marcer, M., Stentoft, P. A., Bjerre, E., Cimoli, E., Bjørk, A., Stenseng, L., and MacHguth, H.: Three decades of volume

680 change of a small Greenlandic glacier using Ground Penetrating Radar, Structure from Motion, and Aerial Photogrammetry, Arctic, Antarct. Alp. Res., 49, 411–425, https://doi.org/10.1657/AAAR0016-049, 2017.

Marti, R., Gascoin, S., Houet, T., Ribière, O., Laffly, D., Condom, T., Monnier, S., Schmutz, M., Camerlynck, C., Tihay, J. P., Soubeyroux, J. M., and René, P.: Evolution of Ossoue Glacier (French Pyrenees) since the end of the Little Ice Age, Cryosphere, 9, 1773–1795, https://doi.org/10.5194/tc-9-1773-2015, 2015.

685 Meier, M. F., Dyurgerov, M. B., Rick, U. K., O'Neel, S., Pfeffer, W. T., Anderson, R. S., et al.: (2007). Glaciers Dominate Eustatic Sea-Level Rise in the 21st Century. Science, 317(5841), 1064–1067. https://doi.org/10.1126/science.1143906, 2007.

Milner, A. M., Khamis, K., Battin, T. J., Brittain, J. E., Barrand, N. E., Füreder, L., et al.: (2017). Glacier shrinkage driving global changes in downstream systems. Proceedings of the National Academy of Sciences, 114(37), 9770–9778.

690 https://doi.org/10.1073/pnas.1619807114, 2017.

Mölg, N. and Bolch, T.: Structure-from-Motion using historical aerial images to analyse changes in glacier surface elevation, Remote Sens (Basel), 9, https://doi.org/10.3390/rs9101021, 2017.

Oliva, M., Ruiz-Fernández, J., Barriendos, M., Benito, G., Cuadrat, J. M., Domínguez-Castro, F., García-Ruiz, J. M., Giralt, S., Gómez-Ortiz, A., Hernández, A., López-Costas, O., López-Moreno, J. I., López-Sáez, J. A., Martínez-Cortizas, A.,

695 Moreno, A., Prohom, M., Saz, M. A., Serrano, E., Tejedor, E., Trigo, R., Valero-Garcés, B., and Vicente-Serrano, S. M.: The

Little Ice Age in Iberian mountains, Earth Sci Rev, 177, 175–208, https://doi.org/https://doi.org/10.1016/j.earscirev.2017.11.010, 2018.

Otero García, J.: Generación automática de malla de elementos finitos en modelos evolutivos de dinámica de glaciares, Universidad Politécnica de Madrid, Madrid, 2008.

700 Otto, J.-C.: Proglacial lakes in high mountain environments, Geomorphology of Proglacial Systems, Springer, 231–247, https://doi.org/10.1007/978-3-319-94184-4_14, 2019.

Palacios, D., Hughes, P., García-Ruiz, J., de Andrés, N. European Glacial Landscapes. The last deglaciation. ELSEIVER. ISBN: 9780323918992. 2022

Otto, J.-C.: Proglacial lakes in high mountain environments, 231–247, https://doi.org/10.1007/978-3-319-94184-4_14, 705 2019.

Pastor Argüello, F.: Determinación del balance anual de masa y movimiento del hielo en el glaciar de la Maladeta. Año hidrológico 2012–2013, Programa ERHIN, 68, 2013.

Pepin, N., Bradley, R. S., Diaz, H. F., Baraer, M., Caceres, E. B., Forsythe, N., et al.: (2015). Elevation-dependent warming in mountain regions of the world., Nature Climate Change, 5(5), 424–430., https://doi.org/10.1038/nclimate2563, 710 2015.

Procházková, B., Engel, Z., and Tomíček, J.: Geometric changes of three glaciers in Dickson Land, central Spitsbergen, during the period 1990–2015, Polar Sci., 20, 129–135, https://doi.org/https://doi.org/10.1016/j.polar.2019.05.004, 2019.

de Reu, J., Bourgeois, J., Bats, M., Zwertvaegher, A., Gelorini, V., de Smedt, P., Chu, W., Antrop, M., de Maeyer, P., Finke, P., van Meirvenne, M., Verniers, J., and Crombé, P.: Application of the topographic position index to heterogeneous 715 landscapes, Geomorphology, 186, 39–49, https://doi.org/https://doi.org/10.1016/j.geomorph.2012.12.015, 2013.

Rabatel, A., Francou, B., Soruco, A., Gomez, J., Cáceres, B., Ceballos, J. L., et al.: (2013). Current state of glaciers in the tropical Andes: a multi-century perspective on glacier evolution and climate change., The Cryosphere, 7(1), 81–102., https://doi.org/10.5194/tc-7-81-2013, 2013.

Rajendra, Y. D., Mehrotra, S. C., Kale, K. V., Manza, R. R., Dhumal, R. K., Nagne, A. D., and Vibhute, A. D.: 720 Evaluation of partially overlapping 3D point cloud's registration by using ICP variant and cloudcompare, Int. Arch. Photogramm. Remote Sens. Spat. Inf. Sci. - ISPRS Arch., XL–8, 891–897, https://doi.org/10.5194/isprsarchives-XL-8-891-2014, 2014.

de Reu, J., Bourgeois, J., Bats, M., Zwertvaegher, A., Gelorini, V., de Smedt, P., Chu, W., Antrop, M., de Maeyer, P., Finke, P., van Meirvenne, M., Verniers, J., and Crombé, P.: Application of the topographic position index to heterogeneous 725 landscapes, Geomorphology, 186, 39–49, https://doi.org/https://doi.org/10.1016/j.geomorph.2012.12.015, 2013.

Revuelto, J., Alonso-González, E., Vidaller-Gayán, I., Lacroix, E., Izagirre, E., Rodríguez-López, G., López-Moreno, J.I.: Intercomparison of UAV platforms for mapping snow depth distribution in complex apline terrain, Cold Regions Science and technology, 190, https://doi.org/10.1016/j.coldregions.2021.103344, 2021.

Rico, I., Serrano, E., Sanjosé, J.J., del Rioi, M.: Responses to Climatic Chages sinde the Little Ice Age in La Paul

Glacier (Central Pyrenees), KREI, Círculo de Estratigrafía Analítica, Gasteiz, 105-116, 2015.

Rico, I., Izagirre, E., Serrano, E., and López-Moreno, J. I.: Superficie glaciar actual en los Pirineos: Una actualización para 2016, Pirineos, 172, e029, https://doi.org/10.3989/Pirineos.2017.172004, 2017.

Rico, I., Magnin, F., López Moreno, J. I., Serrano, E., Alonso-González, E., Revuelto, J., et al.: (2021). First evidence of rock wall permafrost in the Pyrenees (Vignemale peak, 3,298 m a.s.l., 42°46′16″N/0°08′33″W)., Permafrost and Periglacial Processes, 32(4), 673–680., https://doi.org/https://doi.org/10.1002/ppp.2130, 2021.

Riihimaki, C. A., MacGregor, K. R., Anderson, R. S., Anderson, S. P., & Loso, M. G.: (2005). Sediment evacuation and glacial erosion rates at a small alpine glacier., Journal of Geophysical Research: Earth Surface, 110(F3). https://doi.org/https://doi.org/10.1029/2004JF000189, 2005.

del Río, M., Rico, I., Serrano, E. and Tejado, J.J.: Applying GPR and laser scanner techniques to monitor the Ossoue Glacier (Pyrenees). J. Environ. Eng. Geophys., 19(4), 239–248, https://doi.org/10.2113/JEEG19.4.239, 2014.

Shaw, T. E., Ulloa, G., Farías-Barahona, D., Fernandez, R., Lattus, J. M., and McPhee, J.: Glacier albedo reduction and drought effects in the extratropical Andes, 1986–2020, J. Glaciol., 67, 158–169, https://doi.org/DOI: 10.1017/jog.2020.102, 2021.

Shugar, D. H., Burr, A., Haritashya, U. K., Kargel, J. S., Watson, C. S., Kennedy, M. C., Bevington, A. R., Betts, R. A., Harrison, S., and Strattman, K.: Rapid worldwide growth of glacial lakes since 1990, Nat Clim Chang, 10, 939–945, https://doi.org/10.1038/s41558-020-0855-4, 2020.

Snavely, N., Seitz, S. M., and Szeliski, R.: Photo tourism: exploring photo collections in 3D, ACM Trans. Graph., 25, 835–846, https://doi.org/10.1145/1141911.1141964, 2006.

Snook, D. L., & Milner, A. M.: (2001). The influence of glacial runoff on stream macroinvertebrate communities in the Taillon catchment, French Pyrénées., Freshwater Biology, 46(12), 1609–1623., https://doi.org/https://doi.org/10.1046/j.1365-2427.2001.00848.x, 2001.

Solomina, O. N., Bradley, R. S., Jomelli, V., Geirsdottir, A., Kaufman, D. S., Koch, J., McKay, N. P., Masiokas, M., Miller, G., Nesje, A., Nicolussi, K., Owen, L. A., Putnam, A. E., Wanner, H., Wiles, G., and Yang, B.: Glacier fluctuations during the past 2000 years, Quaternary Science Review, 149, 61-90, https://doi.org/10.1016/j.quascirev.2016.04.008, 2016.

Vidaller, I., Revuelto, J., Izagirre, E., Rojas-Heredia, F., Alonso-González, E., Gascoin, S., René, P., Berthier, E., Rico, I., Moreno, A., Serrano, E., Serreta, A., and López-Moreno, J. I.: Toward an ice-free mountain range: Demise of Pyrenean glaciers during 2011–2020, Geophys Res Lett, 48, https://doi.org/10.1029/2021GL094339, 2021.

Vuille, M., Francou, B., Wagnon, P., Juen, I., Kaser, G., Mark, B. G., & Bradley, R. S.: (2008). Climate change and tropical Andean glaciers: Past, present and future. Earth-Science Reviews, 89(3), 79–96. https://doi.org/https://doi.org/10.1016/j.earscirev.2008.04.002, 2008.

Weiss, A.: Topographic position and landforms analysis. In Poster presentation, ESRI User Conference, San Diego, USA, 2001.

Westoby, M. J., Rounce, D. R., Shaw, T. E., Fyffe, C. L., Moore, P. L., Stewart, R. L., and Brock, B. W.: Geomorphological evolution of a debris-covered glacier surface, Earth Surf. Process. Landforms, 45, 3431– 3448, https://doi.org/10.1002/esp.4973, 2020.

Yao, X., Liu, S., Han, L., Sun, M., and Zhao, L.: Definition and classification system of glacial lake for inventory and hazards study, Journal of Geographical Sciences, 28, 193–205, https://doi.org/10.1007/s11442-018-1467-z, 2018.

Yue, X., Li, Z., Zhao, J., Fan, J., Takeuchi, N., and Wang, L.: Variation in albedo and its relationship with surface dust at Urumqi Glacier No. 1 in Tien Shan, China, https://www.frontiersin.org/articles/10.3389/feart.2020.00110, 2020.

Zemp, M., Frey, H., Gärtner-Roer, I., Nussbaumer, S. U., Hoelzle, M., Paul, F., Haeberli, W., Denzinger, F., Ahlstrøm, A. P., Anderson, B., Bajracharya, S., Baroni, C., Braun, L. N., Càceres, B. E., Casassa, G., Cobos, G., Dàvila, L. R., Delgado Granados, H., Demuth, M. N., Espizua, L., Fischer, A., Fujita, K., Gadek, B., Ghazanfar, A., Hagen, J. O., Holmlund, P., Karimi, N., Li, Z., Pelto, M., Pitte, P., Popovnin, V. V., Portocarrero, C. A., Prinz, R., Sangewar, C. V., Severskiy, I., Sigurdsson, O., Soruco, A., Usubaliev, R., and Vincent, C.: Historically unprecedented global glacier decline in the early 21st century, Journal of Glaciology, 61, 745–762, https://doi.org/10.3189/2015JoG15J017, 2015.